ARBS
Annual Review of Biomedical Sciences
ISSN 1806-8774 - http://arbs.biblioteca.unesp.br

Aging Changes of the Urogenital Organs of Rodents as Revealed by Cytochemistry and Radioautography

Tetsuji Nagata
Department of Anatomy and Cell Biology
Shinshu University School of Medicine, Matsumoto, Japan

Abstract

Nagata T. Aging Changes of the Urogenital Organs of Rodents as Revealed by Cytochemistry and Radioautography. ARBS Ann Rev Biomed Sci 2005;7:7-67. For elucidating the morphological changes of aging in macromolecular synthesis such as DNA, RNA, proteins, glucides and enzymes in various organ systems of experimental animals, systematic studies using light and electron microscopic radioautography and cytochemistry in urogenital organs were carried out. The experimental animals mainly used were mainly ddY strain mice at various aging groups from perinatal stage at embryonic day 19, postnatal 1 and 3 days, 1 and 2 weeks, adult stage at 1, 2 and 6 months and senescent stage at 1 and 2 years. The animals were injected with such macromolecular precursors as ^{3}H-thymidine for DNA, ^{3}H-uridine for RNA, ^{3}H -amino acids for proteins, ^{3}H-glucosamine and ^{35}SO4 for glucides. Some enzymes and glycoproteins were also demonstrated by enzyme cytochemistry and immunocytochemistry. The results demonstrated that these precursors were incorporated into various cell types in several urogenital organs at various aging groups from perinatal to adult and senescent stages, showing specific patterns of macromolecular synthesis as well as other enzymes and glycoproteins, respectively. It is concluded that these aging changes could answer to some questions how these organs develop and how they get older.

KEYWORDS: mouse kidney, testis, ovary, uterus, cytochemistry, radioautography, aging

Received: 07/04/05 Accepted: 22/08/05

Correspondence:
Tetsuji Nagata, M.D., Ph.D., Professor Emeritus, Department of Anatomy and Cell Biology, Shinshu University School of Medicine, Matsumoto 390-8621, Japan and Professor, Department of Anatomy, Shinshu Institute of Alternative Medicine, Nagano 390-0816, Japan, Phone: +81-263-35-4600 FAX: +81-263-46-2848, E-mail: nagatas@po.cnet.ne.jp

Financial Support: Grants-in-Aids for Scientific Research from the Ministry of Education, Science, Sports and Culture of Japan Government (No. 001054, 801066, 801031, 501010, 501533, 56870001, 58015046= 02454564) and Grants for Promotion of Characteristic Research and Education from the Japan Foundation for Promotion of Private Schools (1997, 1998, 1999, 2000).

Table of Contents

Introduction

For the purpose of estimating the developmental and aging changes of various organs of experimental animals during the last 50 years, we have developed novel techniques for both light and electron microscopic radioautography and cytochemistry in order to localize intracellular sites of metabolism at cell organelle level, (1) by fixing tissues with chemical fixatives followed by conventional wet-mounting radioautography, (2) as well as to demonstrate soluble compounds by fixing tissues with cryo-fixation followed by dry-mounting radioautography, (3) to demonstrate the sites of incorporations, syntheses and discharge and (4) to estimate the quantities of synthesized molecules of various substances in animals (Nagata & Shimamura, 1958, 1959a,b; Nagata *et al.*, 1961, 1966, 1967, 1969, 1977a,b, 1984, 1986, 1988a,b; Nagata, 1992; 1994a,b,c; 1996a,b,c; 1997a; 1998a; 2001c; 2002a; 2003a,b; 2004a,b,c,d). The localization of silver grains developed by means of conventional radioautography demonstrates only the insoluble radioactive substances bound to the macromolecules fixed in the cell with the chemical fixatives used (Nagata, 1992; 1996a,b; 1997a; 1998a) , while the radioisotopes bound to the small molecules which are not fixed with conventional fixatives can be demonstrated by only cryo-fixation (Nagata, 1994a, 2002a; Nagata & Nawa, 1966a; Nagata & Murata, 1977, Nagata *et al.*, 1977a,b). Conventional radioautographic procedures can be designated as wet-mounting radioautography, since the tissues are processed through both conventional wet treatments fixing in such chemical fixatives as formaldehyde or glutaraldehyde and applying wet radioautographic emulsions to the specimens (Nagata, 1992, 1996ab, 1997a, 1998a, 2002a). In order to demonstrate any soluble radioactive compounds, special techniques are required in accordance with the characteristics of the radioisotopes used for radioautography (Nagata, 1994a; 2002a; Nagata & Murata, 1977). We have applied these methodologies to various organ systems of experimental animals during development and aging, from embryo to postnatal juvenile, mature and senescent stages, using radiolabeled precursors for macromolecular synthesis and reported the aging changes of macromolecular synthesis in some organ systems of mice by means of light microscopic (LM) and electron microscopic (EM) radioautography (RAG). The aging

changes of DNA synthesis in the locomotive (Hayashi *et al.* 1993; Nagata, 1998c), digestive (Chen *et al.*, 1995; Duan *et al.*, 1992; 1993; Jin, 1996; Jin & Nagata, 1995a,b; Ma, 1988; Ma & Nagata, 1988a,b, 1990a; Morita *et al.*, 1994a; Nagata, 1962, 1992, 1993b, 1995a, 2003c, 2004d,e; Nagata & Ma, 2003a,b; Nagata & Usuda, 1985; Nagata *et al.*, 1966a, 1967, 1984, 1986, 2000a), endocrine (Gao *et al.*, 1995a,b; Ito, 1996; Ito & Nagata, 1996; Nagata *et al.* 2000b), urinary (Hanai, 1993; Hanai & Nagata, 1994a,b; Hanai *et al.*, 1993), respiratory (Sun *et al.*,1994; 1995a,b; 1997a; Nagata & Matsumura, 2004), reproductive (Gao, 1993; Gao *et al.*,1994; Li, 1994; Li & Nagata, 1995; Yamada & Nagata, 1992b), circulatory (Murata *et al.*, 1977a,b, 1978; Nagata & Nawa, 1966b; Olea & Nagata, 1992a), nervous (Nagata, 1965; Cui, 1995), and sensory systems (Gao *et al.*, 1992a,b; 1993; Gunarso *et al.*,1997; Kong, 1993; Kong & Nagata, 1994; Kong *et al.*, 1992a; Nagata, 1997a, 1998c; Nagata *et al.*, 1994, 1995; Toriyama, 1995), RNA synthesis in the digestive (Ma & Nagata, 1990b; Nagata & Usuda, 1985; Nagata *et al.*, 1984; 1986), respiratory (Sun, 1995), endocrine (Liang, 1998; Liang *et al.*, 1999), urinary (Hanai & Nagata, 1994a,b), reproductive (Gao, 1993; Li & Nagata, 1995; Yamada & Nagata, 1992a, 1993), circulatory (Olea & Nagata, 1992b), nervous (Nagata, 1966a; Nagata *et al.*, 1999b) and sensory systems (Kong *et al.* 1992b; Gunarso *et al.*, 1996; Nagata & Kong, 1998), or mRNA localization by in situ hybridization (Usuda & Nagata, 1992, 1995; Usuda *et al.*, 1992; Nagata & Kong, 1998; Nagata & Usuda, 1993b). The protein synthesis in the locomotive (Terauchi *et al.*, 1988; Terauchi & Nagata, 1993, 1994), digestive (Ma & Nagata, 2000; Ma *et al.*, 1991; Nagata & Usuda, 1993a; Nagata, 1967, 2000c; Sato, 1978; Sato *et al.*, 1977; Yoshizawa *et al.*, 1974, 1977), respiratory (Sun *et al.*, 1997b), reproductive (Gao, 1993; Yamada, 1993; Oliveira *et al.*, 1991), circulatory (Nagata & Olea, 1999; Olea & Nagata, 2003) and sensory systems (Cui *et al.*, 2000; Toriyama, 1995; Nagata, 1998c, 1999d). The glucide and glycoprotein synthesis in the circulatory (Murata *et al.*, 1979a), digestive (Morita, 1993; Morita *et al.*, 1994a; Nagata & Kawahara, 1999; Nagata *et al.*, 1992; Nagata *et al.*, 1988a, 1992; 1999a; Watanabe *et al.*, 1997, Watanabe & Nagata, 2001), respiratory (Nagata, 2000d), urinary (Johkura, 1996; Johkura *et al.*, 1996) reproductive (Oliveira *et al.*, 1995; Li *et al.*, 1992) and sensory systems (Nagata *et al.*, 1995; Nagata, 2000f) and the lipid synthesis in the digestive system (Nagata *et al.*, 1988b, 1990) were already reported. We have reviewed those results on several organ systems (Nagata, 1993b, 1997a; 1998b, 1999c) or single organ system such as the digestive system (Nagata, 1995a, 2002a), the endocrine system (Nagata *et al.*, 2000b), the respiratory system (Nagata, 2001d) and the sensory system (Nagata, 2000f).

On the other hand, we have also developed other cytochemical methods including (1) several chemical reactions (Duan & Nagata, 1993; Li *et al.*, 1994; Murata *et al.*, 1977c; Nagata, 1997b, 1999a, 2000a, 2001a,b) and enzyme cytochemistry (Murata *et al.*, 1968, 1975; Nagata, 2004a; Nagata & Iwadare, 1984), (2) physical method such as cryotechniques (Nagata, 1994a; Nawa *et al.*, 1965), microspectrophotometry (Nagata, 1966a, 1972a) and X-ray microanalysis (Nagata, 1991, 1993a, 1995d, 2003d, 2004b;

Nagata & Kametani, 2004; Nagata *et al.*, 1998; Kametani, 2002; Kametani & Nagata, 2004; Kametani *et al.*, 2003), and (3) biological methods such as immunocytochemistry (Usuda & Nagata, 1984, 1991, 1995; Usuda *et al.*, 1983, 1986, 1990, 1991a,b,c, 1994, 1995, 1996) and lectin cytochemistry (Hanai *et al.*, 1994a,b; Morita *et al.*, 1994b; Nagata & Kong, 2000).

This paper reviews the results obtained from the urogenital system, especially the urinary system including kidney and urinary tracts and the male and female reproductive system including testis, ovary, uterus and implantation of mice and rats by means of radioautography and cytochemistry which were mainly carried out in our laboratory, as well as referring partly some other related literature from other laboratories. Thus, this review supplements the series of our systematic studies on the aging changes in all the organ systems carried out during these 20 years (Nagata *et al.*, 1984, 1986, 1990; Nagata & Usuda, 1986; Nagata, 1993b, 1995a, 1996c, 1997a, 1998b, 1999c, 2001c, 2002a, 2004b,c).

2. Methods for Demonstrating Chemical Components in Cells and Tissues

The researches in medical and biological sciences aim at clarifying the morphology and functions of human and animal bodies by means of various research methods. The medical and biological sciences dealing with the morphology are anatomy and pathology, while those dealing with the functions are biochemistry and physiology which can be designated as functionology (Nagata, 2004e). Anatomy and pathology deal with the forms and structures of the human and animal bodies, while functionology analyzes the human and animal functions applying chemistry and physics. Recent advances in research methodology in medical and biological sciences have been made at the frontiers between the morphology and functionology, between anatomy-pathology and biochemistry-physiology. This new frontier is designated as histochemistry and cytochemistry which is a science to localize chemical components of cells and tissues on histological sections by using various techniques and analyze the functions based on morphology. I first aimed at studying cytochemistry by developing new special techniques using various principles such as enzyme cytochemistry (Nagata, 1956), microincineration (Nagata *et al.*, 1957b), microspectrophotometry (Nagata, 1961a,b,c), radioautography (Nagata & Shimamura, 1958, 1959a,b; Nagata *et al.*, 1961) and cryo-techniques (Nagata *et al.*, 1969; Nawa *et al.*, 1965, 1969) in 1950-1960s. We have first concentrated to develop methodologies since 1950s to 1960s. However, since these technologies were well developed in 1970-1980s, we then concentrated to apply these special techniques to various kinds of cells and tissues in men and animals. Formerly, I proposed to classify these cytochemical methods into 3 categories, i.e., chemical, physical and biological techniques (Nagata 1995b, 1999b). Recently, the methodology has been well developed to form a new science which should be designated as general histo-and cytochemistry similarly to the general histology. On

the other hand, these techniques should be applied to all the organ systems of men and animals, such as the skeletal, muscular, digestive, respiratory, urinary, reproductive, endocrine, circulatory, nervous and sensory systems. The results of these applications to all the organ systems should be collected to accumulate a new science, i.e. histochemistry of the organs like the histology of the organs. We made efforts to apply these techniques to various organ systems of men and animals since 1970s to the present time (Nagata 1999b, 2001c, 2004a) and collected data from all the organs including the aging process from prenatal, postnatal development to adult and senescent stages. The data include not only 3-dimensional structure of the organs but also the 4-dimensional structure taking the time dimension into account, by labeling cells and tissues in connection with the individual aging. The cytochemical methods will be reviewed by classifying them into 3 categories, chemical, physical and biological methods, according to the principles applied to the methods (Nagata, 1995b; 1999b, 2001c, 2004a).

2.1. Chemical Methods in Cytochemistry

Chemical methods in cytochemistry consist of various chemical reactions such as the historical staining of DNA with Feulgen reaction, staining of proteins with Millon reactions, glucides with PAS reaction, lipids with Sudan and enzymes. The bases of these chemical reactions are well understood. The principles and methods can be divided into two categories, color reactions for light microscopy and dense deposits for electron microscopy.

Various kinds of color reactions for demonstrating various substances have been developed. Among them, we mainly used such color reactions whose intensities and absorbances are parallel with the concentrations of the substances for applying them to microspectrophotometry (Nagata, 1972a). The methods which we used in cytochemistry such as stainings for nucleic acids (Feulgen,1924), proteins (Millon reaction, Sakaguchi reaction), glucides (PAS reaction), lipids (Sudan dyes, Lillie,1944) and enzymes (Gomori,1939; Takamatsu,1938, 1939). Varieties of techniques for demonstrating various enzymes were developed in 1950-1960s so extensively that Pearse (1953) described in his textbook, "Although a few years ago only 2 or 3 enzymes could be demonstrated in the tissues by histochemical means, there are now techniques for at least 18," but after 5 years he (Pearse, 1958) amended the description to "for at least 45." Now in 21st C, this sentence must be amended to read "for at least 200," employing several principles resulting in color reactions such as metal precipitation, azo-dyes, tetrazolium salts, and DAB (diaminobenzidine) osmium. Considering the fact that around 2,100 enzymes were registered by the enzyme committee of the International Union of Biochemistry (1979), the number of enzymes demonstrable cytochemically is too small. Among them, we developed and studied several enzymes such as cytochrome oxidase (Nagata, 1956), urate oxidase (Yokota & Nagata, 1973), catalase (Yokota & Nagata, 1974), acid and alkaline phosphatase, non-specific esterase (Nagata & Murata, 1980), arylsulfatase (Murata *et al.*

1975), lipase (Nagata, 1974) and phospholipase (Nagata & Iwadare, 1984). Several pigments such as melanin, lipofuscin, ceroids, hemoglobin, hemosiderin, bilirubin can also be localized (Nagata *et al.*, 1957a). Varieties of methods for demonstrating inorganic elements, especially metals, by color reactions have been developed since many years. The color reaction produced by union of a dye with a metal or metal salt is called as lake-formation. Numerous techniques exist for the demonstration of metals such as iron, copper, gold, silver, mercury, lead, nickel, aluminum, zinc etc. Among them, color reactions for inorganic iron were frequently used such as Prussian blue or Turnbull blue. However, the specificities of these techniques were mostly unsatisfactory. We have not tried these color reactions so much, but we employed only physical techniques, micro-incineration (Nagata *et al.*, 1957b) and radioautography (Nagata *et al.*, 1977b) for demonstration of inorganic substances.

When electron microscopes were developed and first applied to biology in 1950s, the histologists and pathologists observed thin sections obtained from tissues and cells after electron staining with uranium and lead to increase contrast in specimens. Later in 1960s histochemists who studied localization of chemical components in tissues and cells started to use electron microscopy for localizing in situ chemical reactions by producing electron dense deposits at cell organelle levels. Such field of study on subcellular localization of chemical components of cells was designated as electron microscopic cytochemistry or ultracytochemistry. For example, typical glucides such as glycogen particles contained in various cells can be demonstrated by PA-TCH-SP (periodic acid-thiocarbohydroazide-silver proteinate method, Thiéry, 1967). We improved this method (PA-TCH-SP) and found it to be the most suitable from the viewpoints of reaction specificity, reproducibility, sufficiency of electron density (Murata *et al.*,1977a,b,c). After the staining, fine electron dense reaction products were observed in the cytoplasm of the megakaryocytes and blood platelets of rabbits (Murata *et al.*,1977c) as well as in the mucous granules in the goblet cells in mouse colonic epithelium (Nagata, 2000a, 2001a). Likewise, olyethyleneimine (PEI) stains anionic sites of proteoglycans in various tissues (Sauren *et al.* 1991). We improved the staining method and applied it to several organs. As the results, PEI binding sites in the glomerular extracellular matrices of mouse kidney (Duan & Nagata, 1993) and the hyaline cartilage of mouse trachea (Li *et al.*, 1994) were demonstrated.

On the other hand, various kinds of enzyme activities were first demonstrated by means of the similar techniques used for light microscopy resulting in metal precipitation such as lead deposits for acid phosphatase or lipase (Nagata, 1974). Other metal deposits, such as copper, gold, barium, cerium (Olea & Nagata, 1991, Olea *et al.*, 1991), cadmium, strontium were also used for demonstration of various enzyme activities. Then, electron dense macromolecules produced by azo dyes and tetrazolium salts were used for enzyme cytochemistry. Likewise, varieties of macromolecules, i. e. DNA, RNA, proteins, glucides, lipids and amines were lately demonstrated by labeling with electron dense deposits, for example using enzyme-gold complex localizing DNA and RNA. Among these techniques

we developed and applied several methods for both macromolecules, PEI for glycoproteins (Duan & Nagata, 1993; Li *et al.*, 1994) and PA-TCH-SP for glucides (Murata *et al.*, 1977c), as well as enzymes, such as lipase (Nagata, 1974), phospholipase (Nagata and Iwadare, 1984), catalase (Yokota & Nagata, 1974) and urate oxidase (Yokota & Nagata, 1973, 1977).

With regards to enzyme cytochemistry, the techniques for demonstrating enzyme activity at the light microscopic level were extensively developed in 1950s to 1970s. Then, the techniques for demonstrating enzyme activity at the electron microscopic level, producing electron dense deposits, followed. The principle for demonstrating enzyme activity employs several procedures to produce electron dense deposits such as, metal precipitation, azo-dyes, tetrazolium salts, and DAB (diaminobenzidine) osmium. Among them, we developed and studied several enzymes such as cytochrome oxidase (Nagata, 1956), urate oxidase (Yokota & Nagata, 1974), catalase (Yokota & Nagata, 1974), non-specific esterase (Nagata & Murata, 1980), arylsulfatase (Murata *et al.* 1975), lipase (Nagata, 1974) and phospholipase (Nagata & Iwadare, 1984). Other enzyme activities such as DAB (diaminobenzidine) reaction for peroxisomes, glucose-6-phosphatase (G-6-Pase) activity for endoplasmic reticulum, thiamine pyrophosphatase (TPPase) activity, acid phosphatase activity (AcPase) for lysosomes, cytochrome oxidase activity for mitochondria and ZIO (zinc iodide osmium) reaction for Golgi apparatus were also employed to demonstrate these marker enzymes in respective cell organelles for 3-dimensional observation of cell organelles in thick specimens by high voltage electron microscopy (Nagata, 1995c, 1997b, 1999a, 2000a,e, 2001a,b).

2.2. Physical Methods in Cytochemistry

The principles and methods using physical reactions consist of various physical reactions such as changes of temperature of specimens by means of microincineration or cryo-techniques, and effects of wave-length on absorption such as microspectrophotometry, fluorescence microscopy, confocal laser scanning microscopy, or utilization of radiation such as radioautography and X-ray microanalysis. Using very high temperatures, we studied the inorganic elements in the skin using microincineration modifying Scott technique (Scott & Horning, 1953), by fixing tissues in a mixture of absolute ethanol and neutral formalin, dehydrating, embedding in paraffin, sectioning, and the slides carrying sections were heated to 600°C in an oven, and observed by dark field microscopy (Nagata *et al.*,1957b). To the contrary, very cold temperatures (the cryo-techniques) applied to cytochemistry consist of 3 techniques, (1) cryo-fixation followed by cryo-sectioning, (2) freeze-drying and (3) freeze-substitution (Nagata, 1994a). Varieties of combination of these procedures were successfully utilized to cytochemistry to prevent loss of soluble compounds in cells, displacement of cell constituents by diffusion and denaturation of chemical components especially of enzymes. Historically the cryo-technique to fix and freeze-dry tissues was first introduced by Altmann (1889, 1894). The procedure was later improved by Gersh

(1932) for light microscopy and then for electron microscopy (Gersh, 1956). We used these techniques by designing freeze-drying apparatuses (Nawa *et al.*,1965, 1969) which were applied for both radioautography demonstrating soluble radio-labeled compounds (Nagata *et al.* 1969; Nagata, 1972b, 1994a,b; Nagata & Murata, 1977) and enzyme cytochemistry (Yokota & Nagata, 1973, 1974, 1977) by electron microscopy.

With regards to the wave-length of lights, both visible and invisible lights with various wave lengths from ultraviolet rays to ultrared rays were employed by light microscopy for cytochemistry . Ultraviolet rays were used to observe the absorption bands of both DNA and RNA, while visible rays at definite wavelengths were used for microspectrophotometry of different color reactions. We used microspectrophotometry using both invisible ultraviolet rays and visible spectrum (Nagata, 1966a, 1972a). Using ultraviolet rays, we could measure the nucleic acid contents in respective cells (Nagata, 1966a, 1972a). Microspectrophotometry was originally developed by Caspersson (1936) and widely used to measure the contents of nucleic acids of various cells. We used an Olympus single-beam microspectrophotometer Model MSP-A-IV (Nagata, 1966a).

The radiations due to electromagnetic waves can physically be divided into four: alfa-rays, beta-rays, gamma-rays and X-rays, according to the wave-length from short to long length. Three methods were employed using radiations in cytochemistry, i. e., microradiography, microradioautography and X-ray microanalysis. Microradiography is a technique to observe the picture of small tissue specimens penetrated by radiation from soft X-rays resulting in negative images such as chest X-ray films. The small X-ray films are observed by light microscopy. In cytochemistry, microradiography is used to observe hard tissues such as the bone and the teeth, penetrated by soft X-rays resulting in negative images. We used microradioautography to observe the sliced bone tissues (Nagata, 1995b). By this procedure differences of mineralization in tissue sections can be observed by light microscopy.

Radioautography is a technique to demonstrate the patterns of localization of radioactive substances in various specimens incorporating radioactive compounds (Nagata, 1992, 1994c). The radioautograms can be observed by both light and electron microscopy. The specimen which consists of tissues and cells in contact with the photographic emulsion containing developed silver grains is called radioautograph, while the pattern of silver grains on the radioautograph is called radioautogram and the procedure to produce radioautographs is designated as radioautography. Radioautograph is the autograph produced by radiation. Autograph is a positive picture made by itself. Therefore, the term radioautogram means etymologically the positive picture produced by radiation which is emitted from the object itself resulting in autogram. To the contrary, autoradiograph consists of auto and radiograph. The suffix auto means automatic, while the term radiograph means the picture of the object which is penetrated by rays resulting in negative images such as microradiogram or chest X-ray films. Thus, autoradiograph etymologically means a negative picture of the specimen produced automatically with

radiation emitted from another radiation source away from the specimens which is quiet different from radioautographs (Nagata, 1992, 1994b,c). However, it is now accepted that the both terms, radioautography and autoradiography, are considered to be the synonyms. I had advocated a new concept, named "radioautographology." This new term is the coinage synthesized from radioautography and ology, expressing a new science derived from radioautography. The concept of radioautographology is a science to localize the radioactive substances in the structure of the objects and to analyze and to study the significance of these substances in the structure (Nagata, 1998b, 2002a). The science, radioautographology, can be divided into 2 parts, general radioautographology and special radioautographology. The former deals with the principle and techniques of radioautography, while the latter deals with the application of radiography to various materials (Nagata, 1998b, 2002a). General radioautographology is the technology including all the natural sciences to produce the specimens, which contain radioactive compounds, procedures for tissue preparations and the methods to make tissues contact with the photographic emulsions and to give exposure for a certain period of time to produce the latent images of the radioactive substances in the specimens, then to develop the emulsion to produce the silver metal grains, thus enabling to compare both the specimens and radioautograms in order to learn the localization of radioactive substances in the specimens. We developed the technologies for light (LM) and electron microscopic (EM) radioautography (RAG) and applied them to cell biology and cytochemistry (Nagata, 1996a,b,c, 1997a, 1998a,b, 2002a). The radioactive compounds used in radioautography are mainly composed of inorganic or organic compounds which are artificially labeled with radio-isotopes (RI) and can be incorporated into human or animal bodies by experiments. The radioactivity emitted from the radioactive isotopes are divided into three kinds of rays, i.e., alpha, beta and gamma rays. Among these three rays, the beta ray is the best for radioautography because of its shorter range and the strongest ionization. For radioautography various kinds of RIs are used. Among them, ^{3}H , ^{14}C, ^{35}S and ^{125}I are very often utilized because they can be labeled to various inorganic compounds which are usually used in biological and medical researches. The RI-labeled compounds used for radioautography can be classified into two categories, i. e., the precursors which are incorporated into macromolecules such as nucleic acids (DNA and RNA), proteins, glucides and lipids, and the other target tracers which are small molecular compounds such as hormones, neurotransmitters, vitamins, inorganic substances, drugs and others. The macromolecular synthesis is labeled with ^{3}H-thymidine (for DNA), ^{3}H-uridine (for RNA) amino acids such as ^{3}H-glycine or ^{3}H-leucine (for proteins), ^{3}H-glucose, ^{3}H-glucosamine or $^{35}SO4$ (for glucides) and ^{3}H-glycerol or ^{3}H-fatty acids (for lipids). The experimental animals mainly used in these experiments were ddY strain mice which were maintained and bred in our laboratory. In order to localize the sites of incorporation of radioactive compounds in animal bodies, the compounds which were labeled with specific RIs were usually administered by injections given subcutaneously, intramuscularly, intravenously

or intraperitoneally. In these experiments, we injected the animals intraperitoneally with radioactive precursors for macromolecular syntheses at varying concentrations such as 37-1850 KBq (1-50 μCi)/ gram body weight for both LMRAG and EMRAG or 370-3700 KBq (10-100 μCi)/ g.b.w. depending on the characteristics of the compounds and RIs used. The RI-labeled precursors used in these experiments were ^{3}H-thymidine (Amersham, England, UK, specific activity 877 GBq/mM) for DNA synthesis, ^{3}H-uridine (Amersham, England, 1.11 TBq/mM) for RNA synthesis, d-4,5-^{3}H-leucine (Amersham, England, UK, specific activity 1.04 TBq/mM) or d-^{3}H-proline (Amersham, England, UK, specific activity 877 GBq/mM) for proteins, ^{35}S-sulfuric acid (Amersham, England, UK, specific activity 1.11 TBq/mM) for mucosubstances, d-1,6-^{3}H-glucosamine (New England Nuclear Corporation, Boston, MA, USA, specific activity 185 MBq/mM) for glucides, and ^{3}H-glycerol (New England Nuclear Corporation, Boston, MA, USA, specific activity 740 MBq/mM) for lipids. Embedded tissues in epoxy resin can be used for either light or electron microscopy. For light microscopy thick sections at 2 μm were cut,while ultrathin sections at 100 nm thickness were cut for conventional transmission electron microscope with the accelerating voltage at 100 kV. It is generally accepted that the thinner the section is the better the resolution, but the less the radioactivity it contains and the longer the exposure time for radioautography. We prefer to use semithin sections at 200 nm thickness by observing with high voltage electron microscopy at 400 kV in order to shorten the exposure time (Nagata, 1998a, 2002a). We have developed simple routine standard techniques to demonstrate both soluble and insoluble compounds in various cells and tissues of experimental animals and to quantify the contents of synthesized macromolecules in each cell and cell organelle by both light and electron microscopy. The techniques for microscopic radioautography developed in our laboratory can be divided into two categories, i.e., wet-mounting radioautography for insoluble compounds, such as macromolecular synthesis, and dry-mounting radioautography for soluble compounds, such as small molecular compounds using cryo-techniques including cryo-fixation, cryo-sectioning, freeze-drying, and freeze-substitution (Nagata,1992,1994a,1996b,1998a).

X-ray microanalysis (XMA) is carried out by means of analytical electron microscopes which consist of scanning or transmission electron microscopes equipped with X-ray analyzers (Nagata, 2004). To analyze trace elements in small biological specimens, electron beams (with diameters 5-100 nm) are irradiated at a small spot (with diameters 5-100 nm) and the emitted X-rays are analyzed with either energy dispersive X-ray analyzer (EDX) or wave-dispersive X-ray analyzer (WDX). To analyze the elements in biological specimens, EDX is usually preferred to WDX because all the elements can be detected by EDX. We used transmission analytical electron microscopes equipped with X-ray microanalyzers, i. e., Hitachi H-700 with EMAX-1800E (Horiba, Kyoto, Japan), JEOL JEM 200CX with Kevex 7000-77 (Kevex, U.K.), and JEOL GEM-4000EX with TN-5400 (Tracor-Northern, Middleton, USA) at accelerating voltages from 100 kV to 400 kV. X-ray microanalysis is an excellent method to qualify and quantify basic elements

in biological specimens. We quantified the end products of cytochemical reactions such as Ag in radioautograms, Ce in phosphatase activity, Au in colloidal gold immunostaining or endogenous trace elements such as Zn, Ca, S and Al which originally exist in karyoplasm, cytoplasm or cell organelles of various cells and intracellular matrix after conventional chemical fixation or cryo-fixation. From our results, it was shown that X-ray microanalysis using intermediate high voltage transmission electron microscopy at 300 or 400 kV was very useful resulting in high P/B ratios for quantifying these trace elements in biological specimens (Nagata, 1991, 1993a, 2000b, 2004b).

2.3. Biological Methods in Cytochemistry

Biological methods in cytochemistry employ the biological reactions which can be observed in living organisms both plants and animals. They were later developed than the chemical and physical methods. The biological reaction was first introduced into cytochemistry by Coons *et al.* (1941), when they demonstrated the localization of proteins by the fluorescent antibody method. Later, the lectins obtained from plants were also introduced into cytochemistry as another biological reaction to demonstrate sugar residues of glycoproteins (Sharon and Lis, 1972). We used both techniques to demonstrate proteins and glycoproteins.

With regards to immunocytochemistry, Coons *et al.* (1941) first demonstrated the localization of proteins by the fluorescent antibody method making use of the very high specificity of immune reactions of animals producing antibody in the localization of antigenic proteins. Then, various techniques have been developed by many scientists to label and visualize the localization of antigenic proteins at both light and electron microscopic levels using such markers as fluorochrome (FITC fluorescein isothiocyanate, RITC rhodamine isothiocyanate) and enzymes (HRP horse radish peroxidase) for light microscopy and metals (ferritin or colloidal gold particles) for electron microscopy. Among these techniques, we made use of immunofluorescence and PAP (peroxidase anti-peroxidase) techniques (Usuda & Nagata, 1984, 1991) for light microscopy and developed immunoferritin (Yokota & Nagata, 1973, 1974, 1977) and immunogold techniques for localizing some enzymes for electron microscopy (Usuda & Nagata, 1984, 1991, Usuda *et al.* 1983, 1991a,b,c,1994, 1995,1996).

Lectins were found as carbohydrate-binding proteins obtained from various plants such as *Ricinnus communis* agglutinin from castor beans, concanavalin A from Jack beans, peanut agglutinin from peanut *Arachis hypogaea* or animals such as *Helix pomatin* agglutinin from snails which specifically bind to sugar residues in glycoproteins, such as lactose, mannose, N-acetyl-galactosamine or N-acetyl-glucosamine, respectively. These specificities were applied to demonstrate the localization of these sugar residues by labeling the lectins with such markers as FITC (fluorescein isothiocyanate), HRP (horse radish peroxidase), avidin-biotin, ferritin or gold particles as lectin-conjugates for visualizing the lectin-binding sites by both light and electron microscopy (Roth, 1983; Roth & Binder,

1978). We used some lectin-conjugates to demonstrate several sugar-residues in various specific cells in rat kidney by light and electron microscopy (Hanai *et al.*,1994a,b,c,d). We first studied the compositional changes in glycoconjugates in rat kidney and retina using 16 kinds of biotinylated lectins, followed by ABC (avidin-biotin complex) and DAB method for light microscopy (Hanai *et al.* 1994a,b,c,d). The frozen sections were picked up onto glass slides, and stained with biotinylated lectins followed by ABC (avidin-biotin-complex). As the results, lectin binding sites for specific sugar residues with brown positive reaction can be localized, while control reactions should be negative. Then for electron microscopy, we studied the compositional changes in glycoconjugates in rat kidney and retina using sixteen kinds of biotinylated lectins, followed by protein A-gold technique instead of ABC (avidin-biotin complex) and DAB method for light microscopy (Hanai *et al.* 1994d), slightly modified from Roth (1983). Ultrathin sections were cut and stained by biotinylated lectin conjugates followed by streptavidin colloidal-gold complex. After routine electron staining with uranyl acetate and lead citrate, the positive sites can be demonstrated with gold particle localization (Hanai *et al.* 1994d).

3. Application of Radioautography and Cytochemistry to the Urogenital System

The urogenital system comprises the urinary system and the genital system. Both systems are anatomically and embryologically interwoven, even though they are functionally quite different, because the urinary system excretes urine as the waste products and excess of water, while the genital system keeps the animal race continued by producing two kinds of germ cells. Thus, this review deals with the application of radioautography and cytochemistry to the two systems separately.

4. The Urinary System

The urinary system consists of the paired kidneys and the urinary tract which can be subdivided into the paired ureters and the unpaired urinary bladder and urethra. We have studied the macromolecular synthesis of the kidneys of several groups of aging mice by radioautography as well as some chemical reactions, enzyme cytochemistry, X-ray microanalysis and immunocytochemistry, while the localization of anti-allergic agent was observed in the urinary bladders of adult rats.

4.1. Kidney

The kidneys of mammals consist of the nephrons, which is composed of the renal corpuscles and the uriniferous tubules. The renal corpuscles are composed of the glomeruli which are covered by the Bowman's capsules. They are localized in the outer zone of the kidney, the renal cortex. The uriniferous tubules are composed of two portions, the proximal and distal portions which can further be divided into several segments. The tubules run from the outer zone of the kidney (renal cortex) to the inner zone of the

kidney (renal medulla) and come back to the cortex connecting to the collecting tubules and then to the collecting duct in the medulla of the kidney again.

4.1.1. Chemical Reactions in the Kidney

As for the chemical reactions in the kidney cells, we studied the glomerular extracellular matrices and anionic sites stained with polyethyleneimine (PEI) in aging ddY mice at various ages (Duan & Nagata, 1993). Morphometric data revealed that thickening of the glomerular basement membranes, formation of nodules in the basement membrane and increase in the mesangial matrix were the primary age-related changes in aging mice. There were also electron dense PEI positive deposits in mesangial and subepithelial regions. Quantitative analysis showed that glomerular basement membrane thickness, number and size of nodules and the area of the mesangial matrix were significantly correlated to the age of the animals (Duan & Nagata, 1993).

4.1.2. Enzyme Cytochemistry in the Kidney

We also studied enzyme-cytochemical reactions in kidney cells. Catalase (EC 1.11.1.6. hydrogen peroxidase), as demonstrated by DAB (diaminobenzidin) reaction can be demonstrated in peroxisomes of the uriniferous tubule cells in the kidneys of adult rats (Ohno, 1985; Ohno *et al.*, 1978, 1981, 1982).The number of DAB positive peroxisomes increased in adult rat kidney when the animals were fed on DEHP (diethylhexylphthalate), a peroxisome proliferator, similarly to the hepatocytes of rats. The aging change of catalase activity has not yet been studied. Phospholipase B (EC3.1.1.5. lysolecithin acyl hydrolase) activity was first observed by electron microscopy (Nagata & Iwadare, 1984). The results showed that the reaction products were localized over the terminal portions of smooth surfaced endoplasmic reticulum in the uriniferous tubules of adult mouse kidney. The aging change of this enzyme has not yet been studied. Acid phosphatase (EC 3.1.3.2.) activity in the proximal convoluted tubules of aging mice at various ages was also studied (Olea *et al.*,1991). Eighteen groups of ddY mice, aged from postnatal 1 day, 1 and 2 weeks, 1, 2 and 10 months, were used. The kidney tissues were prefixed in buffered glutaraldehyde, incubated in lanthanade-based glycerophosphate medium containing cerium as the capture reagent for 60 min, postfixed in buffered osmium tetroxide, dehydrated, embedded in Epoxy resin, ultrathin sectioned, observed by electron microscopy (Fig. 1A, 1B). On the electron micrographs, image analysis was carried out to count the number and size of acid phosphatase positive lysosomes in respective groups. The results demonstrated that the number and size of acid phosphatase positive granules (lysosomes) increased significantly from postnatal 1 day to 1 week, reaching a peak at 1 week, then gradually declined until 10 months (Fig. 2A).

4.1.3. X-ray Microanalysis in the Kidney

X-ray microanalysis is a useful method to qualify and quantify basic elements

in biological specimens. We first qualified and quantified endproducts of histochemical reactions such as Ag in radioautographs, Ce in phosphate reaction and Au in colloidal gold immunostaining in various cells and tissues (Nagata, 2004b,c). As for the kidney tissues, we studied the cerium deposits due to acid phosphatase reaction and the aluminum accumulation after aluminum administration in mice.

4.1.3.1. Cerium in the Kidney

The intensity of the reaction products of acid phosphatase (AcPase) in the kidneys of aging mice was quantified by X-ray microanalysis (XMA). The specimens were observed with JEOL JEM-4000EX electron microscope attached with Tracor-Northern TN-5400 EDX microanalyzer, loaded with routine software. The reaction products (precipitate) in lysosomes in the proximal tubule cells of the kidneys at TEM mode for 100 seconds live time at varying accelerating voltages from 100, 200, 300 to 400 kV were observed (Fig. 2B). The localization of cerium deposits was confirmed with two peaks at 4.84 and 5.26 keV, respectively. When the cerium spectra were observed by changing the accelerating voltages at 100, 200, 300 and 400 kV, the intensities of the peaks as well as the backgrounds decreased with increasing accelerating voltages from 100 to 400. However, the average peak to background ratios (P/B) counted at 100, 200, 300 and 400 kV increased from 100 to 400 kV (Olea *et al.* 1991). Therefore, XMA in quantifying cerium contents showing acid phosphatase activity in lysosomes of the uriniferous tubules in the kidneys in several groups of aging mice from newborn day 1 to 10 months were carried out using the accelerating voltage at 400 kV. Six groups of aging ddY mice, each consisting of 3 litter mates of both sexes, from postnatal day 1, 7, 14, month 1, 2 and 10, were used. The kidney tissues were prefixed in cacodylate buffered 2% glutaraldehyde, incubated by cerium (Ce) substrate method, postfixed in osmium tetroxide, embedded in Epoxy resin and sectioned (Olea 1991, Olea and Nagata 1991a,b, 1992a,b). Electron dense Ce deposits were observed in lysosomes of proximal convoluted tubule cells (Fig. 1A, 1B). XMA in TEM mode with beam currents from 2 to 8 nano ampere and an accelerating voltage at 400 kV using a microprobe around 0.5 μm in diameter and an integrating detecting time for 100 sec with a detecting dead time of 30%, by JEOL JEM-4000EX with TN-5400 EDX system was carried out. The localization of Ce deposits was confirmed in 200 lysosomes with two peaks at 4.84 and 5.26 keV, respectively. The X-ray spectra obtained from the lysosomes showing the Ce peak at 4.84keV (Fig. 2B) were used for quantitative analysis. Other peaks were Fe, Ca, Os and Cu, which should be due to the reabsorbed degradation products of hemoglobin, fixative and grid meshes, respectively (Olea *et al.* 1991). It was found that the intensity of AcPase activity as demonstrated by the number and size of lysosomes measured on photographs (Fig. 2A) and the intensity of Ce peak (Fig. 2B) parallelly decreased from day 1 to 10 months in the kidneys of aged mice (Fig. 2C). These results demonstrated that aging changes of AcPase activity as quantified by XMA was related to the development and aging of animals (Olea *et al.* 1991).

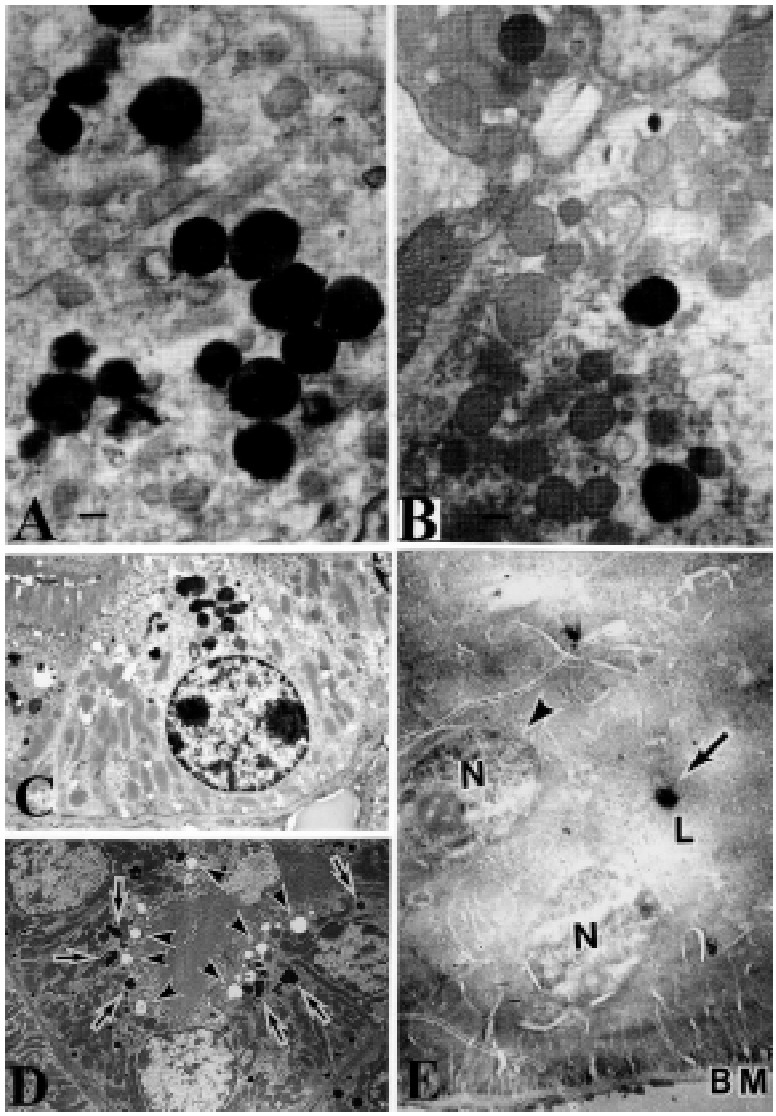

Fig. 1. Chemical and physical reactions in the kidneys of mice as observed by electron microscopy. **(A)** Electron micrographs of proximal convoluted tubule cells of the kidneys of mice at various ages showing intense acid phosphatase (AcPase) activities by Ce substrate method without electron staining. A tubule cell of a juvenile mouse at postnatal week 1, showing AcPase activity in many lysosomes. From Olea *et al.* (1991); **(B)** A tubule cell of a senescent mouse at postnatal month 10, showing AcPase activity in only a few lysosomes. From Olea *et al.* (1991); **(C)** Electron micrograph of proximal convoluted tubule cells of the kidney of a mouse at 6 weeks after birth and administered orally with Al for 2 weeks, fixed in glutaraldehyde and osmium tetroxide, embedded in Epoxy resin, stained doubly with uranyl acetate and lead citrate. In the cytoplasm of the tubule cells, many lysosomes with high electron density can be seen. x7,000. From Kametani (2002); **(D)** Electron micrograph of a proximal convoluted tubule cell of the kidney of a mouse at 9 weeks after birth and administered orally with Al for 9 weeks, fixed with only glutaraldehyde, embedded in Epoxy resin, stained with uranyl acetate and lead citrate. Many electron dense lysosomes (arrows) and small electron transparent vacuoles (arrow heads) are observed in the apical cytoplasm near the urinary lumen. x5,000. From Kametani *et al.* (2003); **(E)** Electron micrograph of a proximal convoluted tubule cell of the kidney of a mouse at 9 weeks after birth and administered orally with Al for 9 weeks, fixed with only glutaraldehyde, embedded in Technovit resin, stained with only uranyl acetate. Because of the procedures employed, the electron densities of respective cell organelles are less as compared with the conventional procedure, but the ultrastructures of nuclei (N), lysosomes (L) and basement membrane (BM) can be recognized. x8,000. From Kametani *et al.* (2003).

4.1.3.2. Aluminum in the Kidney

Spencer *et al.* (1995) monitored Al (aluminum) levels in the plasma and urine of rats after intravenous administration of aluminum citrate or chloride by atomic absorption spectroscopy as well as the aluminum content at the cellular and subcellular level by XMA. They found that aluminum concentrations were significantly higher in the plasma and urine of rats administered with aluminum than controls without administration as demonstrated by atomic absorption spectroscopy. They also found that significant amounts of aluminum were found in cytoplasm and mitochondria of proximal convoluted tubule cells of rats given aluminum citrate, but not in nuclei or lysosomes of these cells. Aluminum levels were not detectable in control kidneys, in proximal tubule cells after aluminum chloride administration or distal tubule cells after either aluminum citrate or chloride treatment. In human patients aluminum has been proved to be toxic, mainly in chronic renal insufficiency. Most cases of aluminum intoxication occur during hemodialysis due to treatment of aluminum-containing drugs. Several human cases were reported with visceral manifestations of aluminum deposition in multidialysed patients. In such cases, light and polarization microscopy examinations and XMA revealed amorphous, extracellular aluminum deposits in various parenchymal organs causing failure of heart, lung and kidney functions (Patonai *et al.* 1996).

We first studied several adult ddY mice 4 weeks after birth which were intraperitoneally injected with aluminum chloride. The duodenum, the liver, the kidney and the cerebral cortex tissues were examined by both aluminon staining with light microscopy and XMA at various accelerating voltages from 100 to 400 kV with analytical electron microscopy. From the results obtained, 1.0 mm thick sections observed at 300kV resulted in the highest peak-counts to background ratios and were shown to be the most suitable for XMA (Kametani, 2002). As for the kidneys by light microscopic aluminon staining, no positive reaction was observed. By TEM, however, many lysosomes with high electron density were observed in the apical cytoplasm of the proximal convoluted tubule cells of the kidneys (Fig. 1C), which resulted in the spectra showing high Al peaks by XMA (Fig. 3). The results revealed that orally administered Al was absorbed from the gastrointestinal tract and re-absorved in the proximal convoluted cells. Then, we studied 9 groups of ddY mice at various aging stages from newborn to adult, each consisting of 3 litter mates, from postnatal weeks 1, 3, 5, 7, 9, 11, 13, 15 and 17 (Kametani *et al.*, 2003). They were administered orally with deionized water containing 2% aluminum chloride (AlCl3) at pH 2.5, ad libitum immediately after birth until 17 weeks. As normal control animals, some animals were administered with only deionized water without aluminum chloride. The animals were sacrificed at each administration period and the kidney tissues were fixed either only in 2.5% glutaraldehyde in phosphate buffer or doubly in glutaraldehyde and osmium tetroxide, dehydrated in ethanol, substituted in propylene oxide and embedded in Technovit VL7200 resin (Meiwa Co., Tokyo, Japan). Thick sections at 1.0 mm were

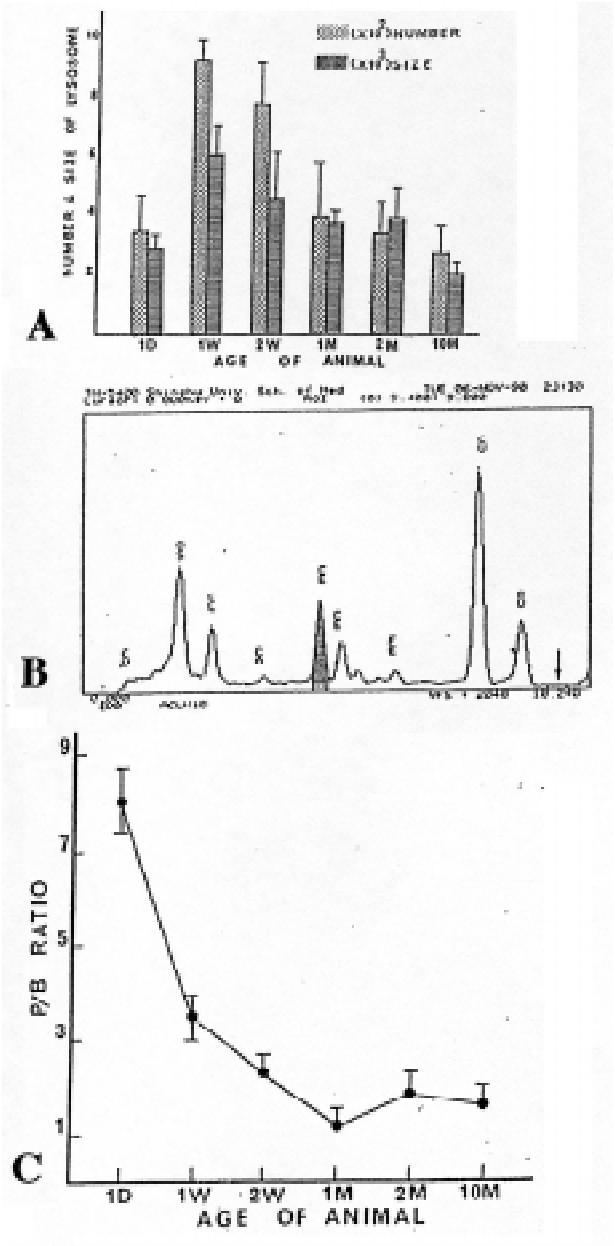

Fig. 2. Aging changes of proximal convoluted tubule cells of the kidneys of mice at various ages demonstrating acid phosphatase (AcPase) activities by Ce substrate method. From Olea *et al.* (1991).
(A) Histogram showing the average size and number of AcPase positive lysosomes in the proximal convoluted tubule cells of mice at various ages. Mean ± standard deviation; **(B)** X-ray spectrum obtained from one of the lysosomes in a tubule cell of a mouse at postnatal day 1 observed by analytical electron microscopy at accelerating voltage of 300kV. The main spectral line of cerium (shaded) was determined at L=4.84 keV. The arrow indicates the point at which the background spectrum was determined; **(C)** Transitional curve demonstrating the relation between the P/B ratios of AcPase activity (ordinate) and the aging of animals (abscissa).

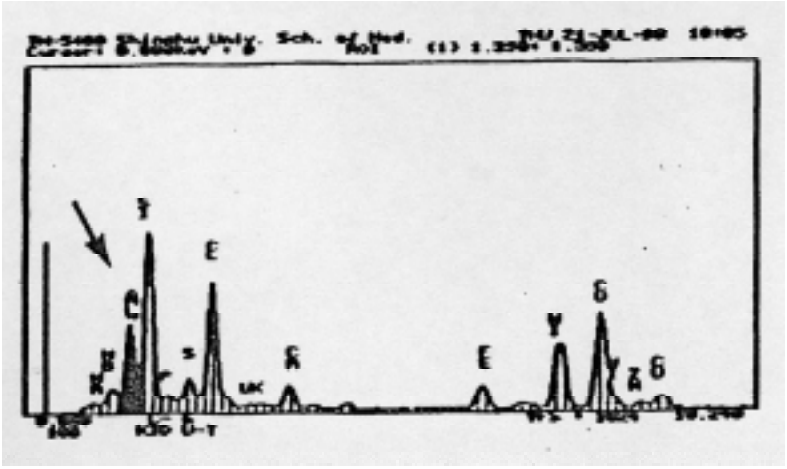

Fig. 3. X-ray spectrum obtained from a lysosome of a proximal convoluted tubule cell of a 6 week old mouse administered orally with Al for 2 weeks, fixed with glutaraldehyde and osmium tetroxide, embedded in Epoxy resin, stained doubly with uranyl acetate and lead citrate, which shows an Al peak (arrow). From Kametani (2002).

cut, mounted on nylon grids (Oken, Tokyo, Japan), stained with only uranyl acetate, observed and analyzed in a JEOL JEM-4000EX TEM equipped with a TN-5400 EDX microanalyzer (Tracor-Northern, Wisconsin, USA) at an accelerating voltage of 300kV. The results showed that many high electron dense lysosomes were observed in the proximal convoluted cells of the Al administered mice which increased from newborn to 17 weeks after birth by conventional electron microscopy (Fig. 1D). Another electron micrograph after fixation with only glutaraldehyde, embedded in Technovit resin, sectioned and stained with only uranyl acetate in order to avoid the osmium and lead shows the highly electron dense lysosomes and less electron dense structures in the nucleus in the proximal convoluted tubule cell of the mouse kidney administered with Al for 9 weeks (Fig. 1E). The EDX spectra obtained from the lysosomes (Fig. 4A) and the nuclei (Fig. 4B) of the tubule cells showed not only Al but also Na, Si, P, S, Cl, U, K, Ca, Fe and Cu. The transitional changes of P/B ratio of Al with administration periods in both lysosomes and nuclei of either administered with Al or not for 17 weeks are shown in Fig. 5. The highest peak of Al P/B ratio was at the period after Al administration for 1 week. Comparing the P/B ratios of Al in the lysosomes between the two groups of the experimental animals with Al and without Al, the former were higher than the latter at respective administration periods. The stochastical analysis on the significant differences between the quantities of Al in the lysosomes of the kidneys of mice in the two experimental groups with and without Al, as well as the transition during the administration, were calculated. The results showed that the significance of Al administration in the lysosomes and the nuclei as well as the significance of administration periods were high (Kametani *et al.*, 2003). Small amount of Al in the tissues of the kidneys, duodenums and livers of the mice fed with Al was also demonstrated by energy spectroscopic imaging with electron loss spectroscopy (EELS) which is more sensitive for elemental analysis than EDX analysis (Kametani & Nagata, 2004).

4.1.4. Radioautography in the Kidney

As for another physical reaction, radioautographic studies on macromolecular syntheses were extensively carried out in our laboratory. The DNA synthesis using ^{3}H-thymidine was carried out in three groups of ddY mouse embryos from prenatal day 13 (Fig. 6A), day 15 (Fig. 6B) to day 19 *in vitro*, as well as in several groups of perinatal mice from prenatal day 19 to postnatal day 1, 8, 30, 60 and 365 (1 year) *in vivo* (Hanai, 1993; Hanai & Nagata, 1994a,b). The labeling indices showing DNA synthesis by LMRAG (Hanai, 1993) in glomeruli (28 to 32%) and uriniferous tubules (31 to 33%) in the superficial layer were higher than those of glomeruli (10 to 12%) and tubules (8 to 16%) in the deeper layer from the late fetal to the suckling period (Fig. 7A). Then they decreased with aging from weanling to adult and senescence (Fig. 7B). Electron microscopic radioautography (EMRAG) revealed the same results (Hanai & Nagata, 1994a). On the other hand, the incorporation of ^{3}H-thymidine was observed in mitochondrial matrix of

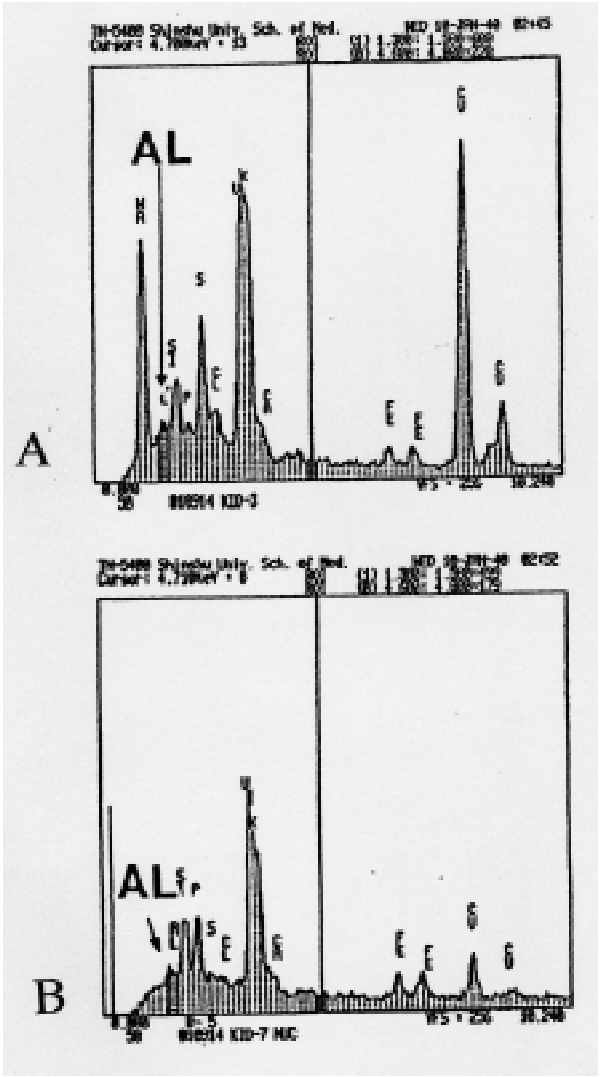

Fig. 4. X-ray spectra obtained from a proximal convoluted tubule cell of a mouse at 9 weeks after birth and administered orally with Al for 9 weeks, fixed with only glutaraldehyde, embedded in Technovit resin, stained with only uranyl acetate as shown in Fig. 1E. From Kametani *et al.* (2003).
(A) X-ray spectra obtained from a highly electron dense lysosome (arrow) of a proximal convoluted tubule cell; **(B)** X-ray spectra obtained from the nucleus (arrow head) of a proximal convoluted tubule cell.

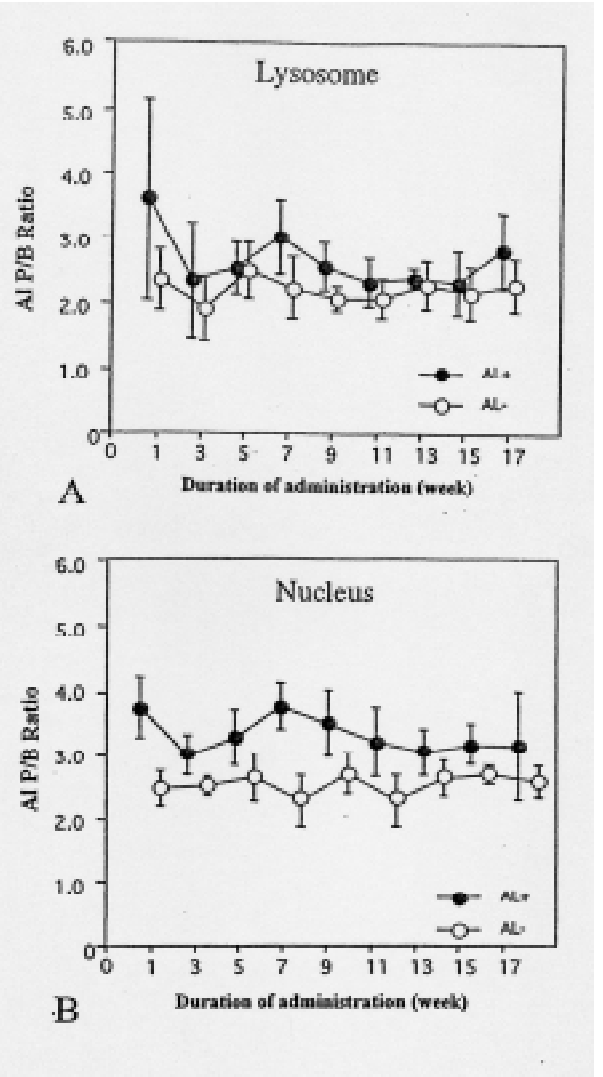

Fig. 5. Transitional changes of P/B ratios of Al obtained from the lysosomes and the nuclei of proximal convoluted tubule cells of mice administered with or without Al chloride from 1 to 17 weeks. The P/B ratios of the Al administration groups were significantly higher than the non-Al groups. From Kametani *et al.* (2003). **(A)** Relationship between the P/B ratios of Al obtained from lysosomes (ordinate) and the duration of Al administration (abscissa); **(B)** Relationship between the P/B ratios of Al obtained from nuclei (ordinate) and the duration of Al administration (abscissa).

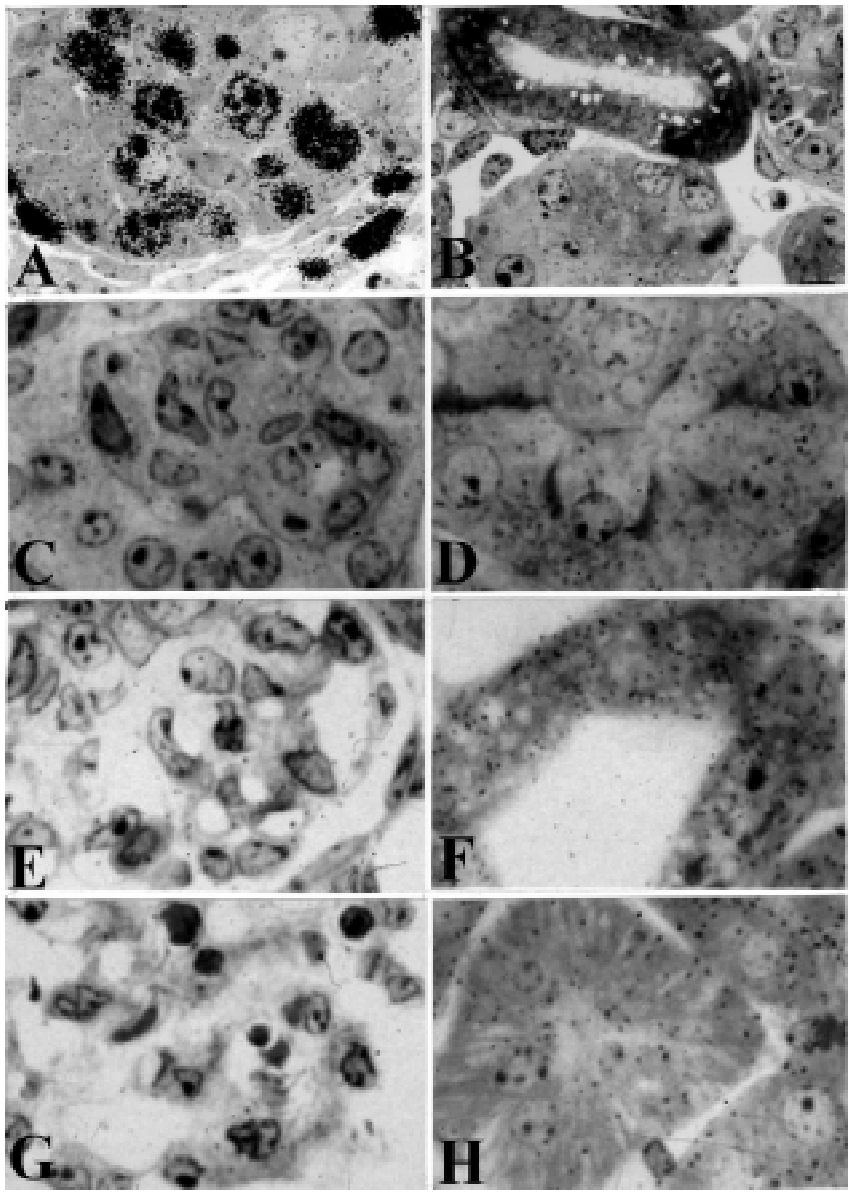

Fig. 6. Light microscopic radioautograms of various cells from the kidneys of mice after administrations of RI-labeled precursors at several aging stages. **(A)** LMRAG of the metanephros of a mouse embryo at day 13.5 of the gestational stage, labeled with ^{3}H-thymidine in vitro. Many labeled nuclei can be seen. x1,600. From Hanai (1993); **(B)** LMRAG of the metanephric cortex of a mouse embryo at day 15.5 of the gestational stage, labeled with ^{3}H-thymidine in vitro. Less nuclei are labeled. x1,300. From Hanai (1993); **(C)** LMRAG of a renal corpuscle in the metanephros of a mouse embryo at day 19 of the gestational stage, injected with ^{3}H-glucosamine *in vivo*. Silver grains are observed over the nuclei and cytoplasm. x1,000. From Johkura (1996); **(D)** LMRAG of renal tubules in the metanephros of a mouse embryo at day 19 of the gestational stage, injected with ^{3}H-glucosamine *in vivo*. Silver grains are observed over the nuclei and cytoplasm. x1,000. From Johkura (1996); **(E)** LMRAG of a renal corpuscle in the kidney of a newborn mouse at postnatal day 1, injected with ^{3}H-glucosamine *in vivo*. Silver grains are observed over the nuclei and cytoplasm. x1,000. From Johkura (1996); **(F)** LMRAG of renal tubules in the kidney of a newborn mouse at postnatal day 1, injected with ^{3}H-glucosamine *in vivo*. Many silver grains are observed over the nuclei and cytoplasm. x1,000. From Johkura (1996); **(G)** LMRAG of a renal corpuscle in the kidney of a newborn mouse at postnatal day 8, injected with ^{3}H-glucosamine *in vivo*. Silver grains are observed over the nuclei and cytoplasm. x1,000. From Johkura (1996); **(H)** LMRAG of renal tubules in the kidney of a senescent mouse at postnatal day 3, injected with ^{3}H-glucosamine *in vivo*. Many silver grains are observed over the nuclei and cytoplasm. x1,000. From Johkura (1996).

cultured kidney cells from chickens and mice in vitro demonstrating mitochondrial DNA synthesis by EMRAG (Nagata *et al.*, 1967).

When the kidneys of several groups of aging mice from embryo to postnatal 1 year were radioautographed with 3H-uridine both i*n vitro* and *in vivo*, RNA synthesis was observed in all cells of the kidneys at various ages (Hanai & Nagata, 1994b). The numbers of silver grains demonstrating the incorporation of ^{3}H-uridine in glomeruli (34.6 per cell) and uriniferous tubules (56.4 per cell) were higher in the superficial layer than those (15.6 and 18.6 per cell) in the deeper layer at embryonic day 15 and decreased gradually with aging (Fig.8). These results revealed that the nucleic acid syntheses, both DNA and RNA, were changed according to the aging of animals.

The incorporations of ^{3}H-glucosamine in the kidneys of aging mice in 6 groups were demonstrated by LM and EM RAG (Johkura, 1996, Johkura *et al.*, 1996). On the radioautograms the numbers of silver grains in both glomeruli (Fig. 6C) and uriniferous tubules (Fig. 6D) were less in the embryonic stage, but increased postnatally in both glomeruli (Fig. 6E) and tubules (Fig. 6F) on day 1, then decreased from day 8 (Fig. 6G, 6H) to senescence. The incorporations of glucosamine into the renal corpuscles and uriniferous tubules in respective aging groups were quantitatively analyzed by grain counting. The results showed that glucide synthesis in the kidney cells increased from embryonic stage to postnatal newborn stage at day 1 and decreased to the senescence at year 1 (Fig. 9), showing the change with aging of animals (Johkura, 1996, Johkura *et al.*, 1996).

4.1.5. Immunocytochemistry in the Kidney

With regards to the biological reactions, several kinds of immunostaining at both LM and EM levels, were carried out in our laboratory. The immunocytochemical localization of retinal binding protein stained by PAP method was observed in the lysosomes of the proximal tubules of the human kidneys (Usuda *et al.*, 1983). The localization of D-amino acid oxidase stained by PAP method was found in the fine cytoplasmic granules of the proximal tubules of rat kidney by LM, while protein A-gold particles were exclusively confined in peroxisomes in the proximal tubules by EM. The fine localization of gold particles was found only in the central core matrix of the peroxisomes, which suggested a specific intra-organellar localization of this enzyme (Usuda *et al.*, 1986).

The proliferating cell nuclear antigen (PCNA/cyclin) immunohistochemistry was also studied in the kidneys of several aging groups of mice (Hanai, 1993; Hanai & Nagata, 1994a,b), similarly to the aging changes of the DNA synthesis by ^{3}H-thymidine radioautography. The PCNA/cyclin positive indices were analyzed in six groups of ddY mice from prenatal day 19 to postnatal 1 year. The indices were decreased from fetal day 19 to postnatal day 1, 5, week 3, and month 2, due to aging in both glomeruli (28 to 32%) and uriniferous tubules (31 to 33%) in the superficial layer. The indices were higher in the superficial layer than those glomeruli (10 to 12%) and tubules (8 to 16%) in the deeper

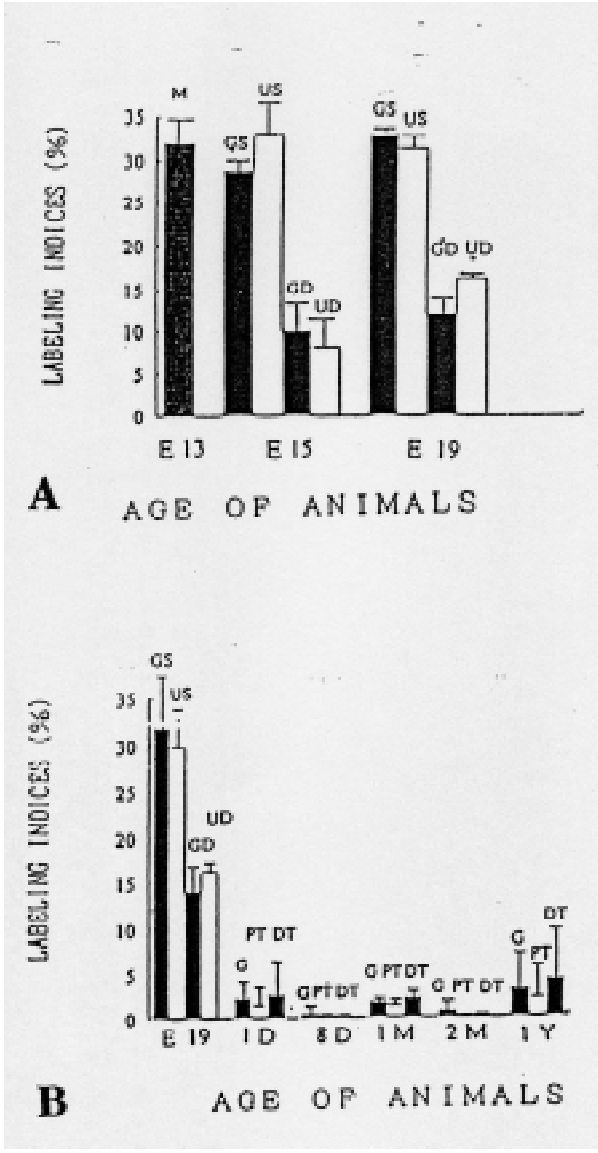

Fig. 7. Histograms showing the labeling indices of mouse kidney cells, labeled with ^{3}H-thymidine at various ages. From Hanai & Nagata (1994a). **(A)** Labeling indices of glomeruli and uriniferous tubules of the kidneys of mouse embryos from fetal day 13 to 19, labeled with ^{3}H-thymidine *in vitro*;
(B) Labeling indices of glomeruli, proximal tubules and distal tubules in the kidneys of mouse embryos from prenatal day 19 to postnatal day 365 (1 year), labeled with ^{3}H-thymidine *in vivo*. Abbreviations to the figures. GS; glomeruli of the superficial layer, US; uriniferous tubules of the superficial layer, GD; glomeruli of the deeper layer, UD; uriniferous tubules of the deeper layer, G; glomeruli, PT; proximal tubules, DT; distal tubules.

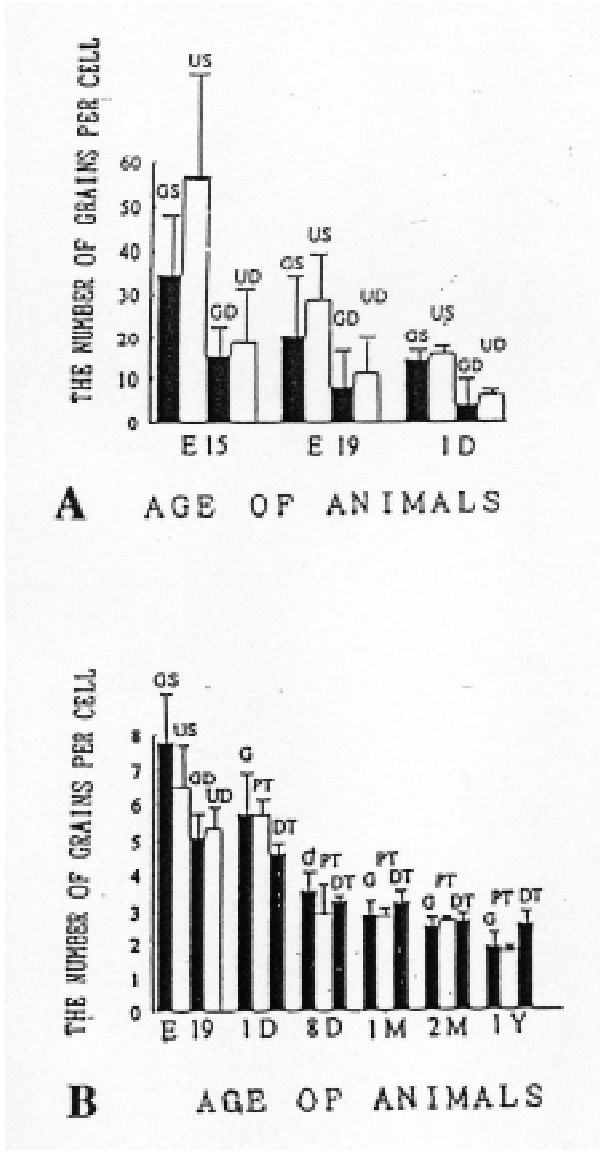

Fig. 8. Histograms showing the average grain counts of mouse kidney cells, labeled with ^{3}H-uridine at various ages. From Hanai & Nagata (1994a). **(A)** Average grain counts of glomeruli and uriniferous tubules of mouse kidneys from embryonic day 15 to postnatal day 1, labeled *in vitro*; **(B)** Average grain counts of glomeruli, proximal tubules and distal tubules in mouse kidneys from prenatal day 19 to postnatal day 365 (1 year), labeled *in vivo*. Abbreviations to the figures. GS; glomeruli of the superficial layer, US; uriniferous tubules of the superficial layer, GD; glomeruli of the deeper layer, UD; uriniferous tubules of the deeper layer, G; glomeruli, PT; proximal tubules, DT; distal tubules.

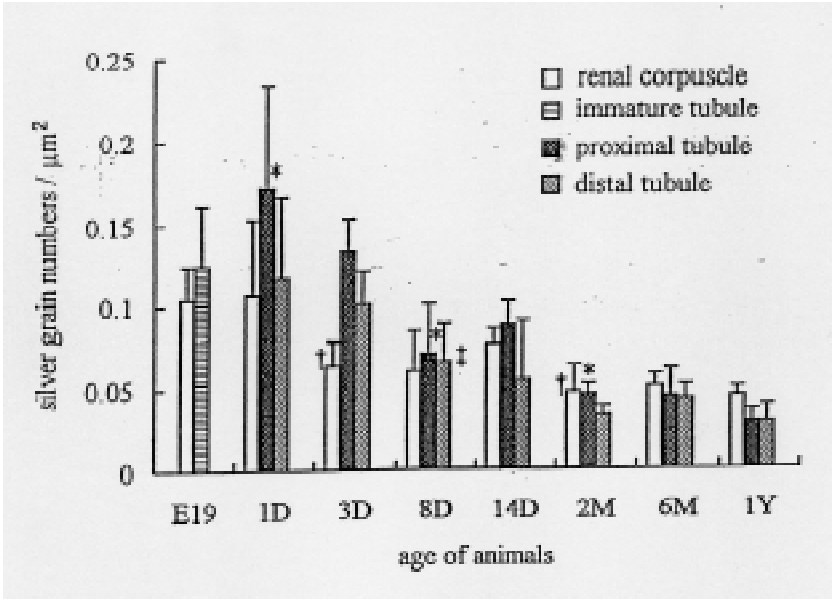

Fig. 9. Histogram showing the average grain counts of mouse kidney cells (ordinate), labeled with ^{3}H-glucosamine *in vivo*, in relation to aging (abscissa). Mean ± standard deviation. *Significantly different from the prior age group at $P<0.01$. From Johkura *et al.* (1996).

Fig. 10. Transitional curves showing the aging changes of PCNA/cyclin positive ratios (%) in mouse kidney cells immunostained with PCNA/cyclin antibody from prenatal day 19 to postnatal 11 months. Relationship between the PCNA/cyclin positive cells (ordinate) and the aging of animals (abscissa). The dotted lines show the positive ratios of the glomeruli and the solid lines the uriniferous tubules in the renal cortex. Mean ± standard deviation. From Hanai *et al.* (1993).

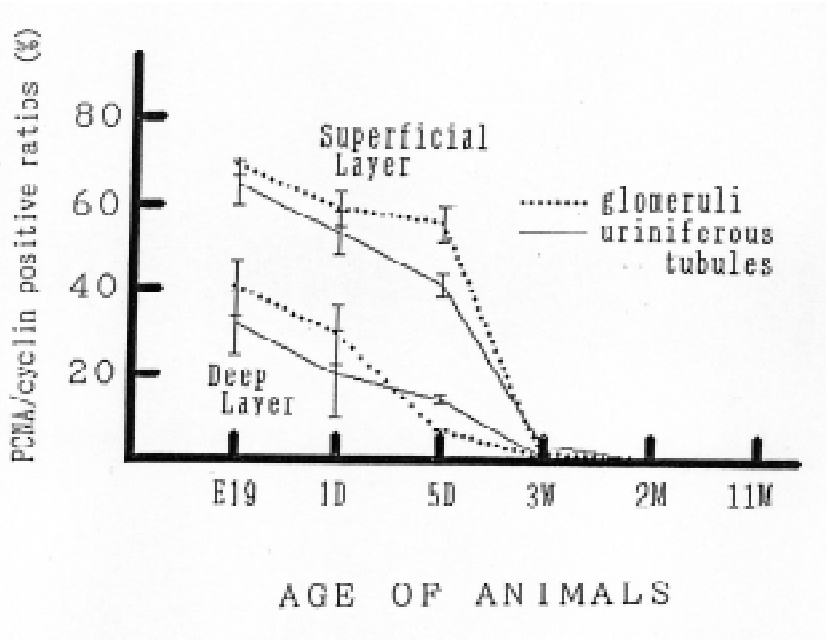

layer from the late fetal to the suckling period (Fig. 10). Then they decreased with aging from weanling to senescence.

4.1.6. Lectin Cytochemistry in the Kidney

On the other hand, lectin cytochemistry was applied in order to demonstrate compositional changes in glycoconjugates in mouse kidney cortex due to aging (Hanai *et al.*, 1994a,b,c,d). Mouse kidney tissues of prenatal and postnatal aging groups from fetal day 19 to postnatal 10 months were fixed in paraformaldehyde, cryosectioned and stained with 16 kinds of biotinylated lectins, followed by ABC (avidin-biotin-peroxidase complex) staining. The reaction products with WGA (wheat germ agglutinin, *Triticum vulgaris*) which is specific for GalNAc (N-acetyl-D-glucosamine) were localized in the glomerular podocytes and tubule basement membranes of adult cortex. The localizations of other lectins (ConA, DSA, SSA, ABA, LCA, PHA-E4, RCA60, and RCA20) were different. The main localization of reaction products for ConA (*Concanavalia ensiformis*), which is specific for Man (mannose), MM (methyl-a-D-mannoside) and MG (methyl-a-D-glucoside), in adult cortex was in the cytoplasm and brush borders of proximal tubules and the blood capillaries of glomeruli. The localization for SSA *(Sambucus sieboludiana),* which is specific for lactose, in the blood capillaries of glomeruli and tubule basement membrane. The reaction products for DSA (*Datura stroamonium*, specific for chito-oligosaccharide), ABA (*Agaricus bisporus*, specific for Gal and GalNAc), LCA (*Lens culinaris*, specific for Man, MM, MG), PHA-E4 (*Phaseolus vulgaris E4*, specific for GalNAc), RCA60 (*Ricinus communis* 60, specific for D-galactose and lactose), and RCA120 (*Ricinus communis* 120, specific for D-galactose and lactose) were localized in the brush borders of proximal tubules and the blood capillaries of glomeruli. The reaction products for Lotus (*Lotus tetragonolobus*, specific for fucose) were localized in the cytoplasm and the brush borders of proximal tubules of adult cortex. The deep layer of the cortex was consistently positive for Lotus during development and aging. Other four lectins MAM, PNA, SBA and PHA-L4 (*Maackia amurensis, Peanut arahis huposaea,* Soybean glycine max, *Phaseolus vulgaris E4*) showed similar changes in the localization of reaction products, blood capillaries of glomeruli and brush borders of proximal tubules. The localization for UEA-I (*Ulex europaeus I*, specific for fucose) was consistently negative in developing and aging kidney cortex but only positive in the erythrocytes in adult cortex. These results demonstrated aging changes in glycoconjugates in the kidney cells.

4.2. Urinary Tract

The urinary tract is composed of the paired ureters, unpaired urinary bladder and urethra. We studied the urinary bladders of rats by LMRAG..

4.2.1. Urinary Bladder

Localization of an anti-allergic agent, tranilast, was studied in the urinary

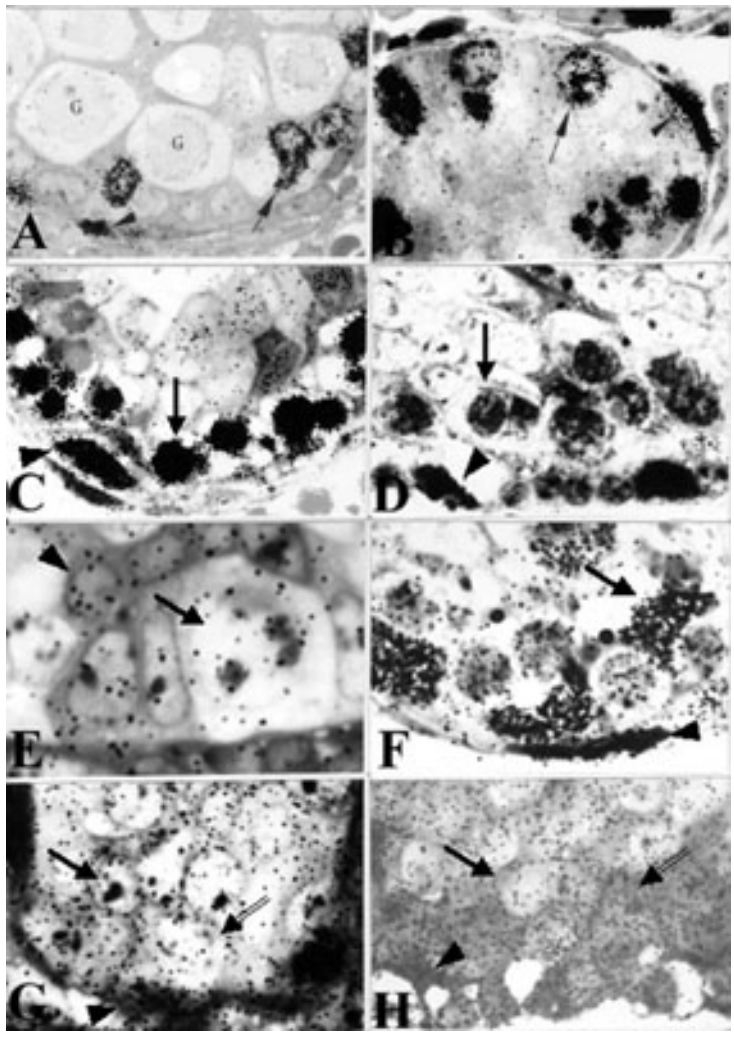

Fig. 11. Light microscopic radioautograms (LMRAG) of the male reproductive system. **(A)** LMRAG of the testis of a male mouse embryo at fetal day 19, labeled with ^{3}H-thymidine *in vitro*. Note that several spermatogonia (arrow) and myoid cells (arrowhead) are labeled with many silver grains showing DNA synthesis but no spermatocytes (G) are labeled. x1,100. From Nagata (2002a); **(B)** LMRAG of the testis of a male mouse embryo at postnatal day 7, labeled with ^{3}H-thymidine *in vitro*. Several spermatogonia (arrow) and myoid cells (arrowhead) are labeled with silver grains showing DNA synthesis. x1,300. From Nagata (2002a); **(C)** LMRAG of the testis of a male mouse at postnatal month 1, labeled with ^{3}H-thymidine *in vitro*. Several spermatogonia (arrow) and a myoid cell (arrowhead) are labeled with silver grains. x1,000. From Nagata (2002a); **(D)** LMRAG of the testis of a male mouse at postnatal year 1, labeled with ^{3}H-thymidine *in vitro*. Many spermatocytes (arrow) and a few myoid cells (arrowhead) are labeled with silver grains. x1,000. From Nagata (2002a); **(E)** LMRAG of the testis of a male mouse at postnatal day 1, labeled with ^{3}H-uridine *in vitro,* showing RNA synthesis. Several silver grains are observed over the nuclei and cytoplasm of Sertoli cells (arrow) and spermatocytes (arrowhead) showing RNA synthesis. x2,000. From Nagata (2002a); **(F)** LMRAG of the testis of a male mouse at postnatal month 6, labeled with ^{3}H-uridine in vitro. Many silver grains are observed over the nuclei and cytoplasm of spermatocytes (arrow) and myoid cells (arrowhead). x1,500. From Nagata (2002a); **(G)** LMRAG of the testis of a male mouse at postnatal day 1, labeled with ^{3}H-leucine *in vitro* showing protein synthesis. Several silver grains are observed over the nuclei and cytoplasm of Sertoli cells (double arrow), spermatocytes (arrow) and myoid cells (arrowhead) showing protein synthesis. x1,000. From Nagata (2002a); **(H)** LMRAG of the testis of a male mouse at postnatal 1 year, labeled with ^{3}H-leucine *in vitro*. Many silver grains are observed over the nuclei and cytoplasm of Sertoli cells (double arrow), spermatocytes (arrow) and myoid cells (arrowhead). x1,000. From Nagata (2002a).

bladders of young adult rats by LMRAG. Tranilast is a synthetic anti-allergic agent, synthesized by Kissei Pharmaceutical Co.(Matsumoto, Japan). Its chemical structure is N-(3, 4-dimethoxycinnamoyl) anthranilic acid, which was labeled with ^{3}H by NEN, Boston, MA, USA (Nagata *et al.*, 1986; Nishigaki *et al.*, 1987, 1990). The urinary bladders of adult Wistar rats were investigated by LMRAG after oral administration of ^{3}H-tranilast. It was found that this agent specifically localized over the transitional epithelial cells and endothelial cells of the veins in the mucosa for a long time (Momose *et al.*, 1989; Nishigaki *et al.*, 1990). These results suggested the relationship between the histopathology of the cystitis observed clinically after the administration of the drug in human patients (Nishigaki *et al.*, 1990).

5. The Reproductive System

The reproductive system consists of the male reproductive system (male genital organs) and the female reproduciteve system (female genital organs). We studied both male and female reproductive systems of several groups of ddY mice in aging by both LM and EMRAG using macromolecular precursors.

5.1. Male Reproductive System

The male reproductive system (or the male genital organ) is composed of the testis and its excretory ducts such as ductuli efferentes, ductus epididymidis, ductus deferens, ejaculatory ducts, as well as the auxiliary glands and the penis. Among these organs, the testis was the main target of our scientific interests.

5.1.1. Testis

The testis is mainly composed of the testicular lobules which is surrounded by a thick capsule, the tunica albuginea. The testicular lobules consist of many seminiferous tubules which are connected to the rete testis and to the epididymis by many ductuli efferentes. The seminiferous tubules consist of seminiferous epithelium composed of the supporting cells or Sertoli cells and the spermatogenic cells including several types of cells, spermatogonia, spermatocytes, spermatids and spermatozoa which are surrounded by the basal lamina and myoid cells. The spaces between the seminiferous tubules are filled with connective tissues or the interstitial tissues which include Leydig cells. We studied the DNA, RNA and protein syntheses of these cells, the spermatogenic cells, Sertoli cells, myoid cells and Leydig cells by LM and EMRAG using ^{3}H-labeled macromolecular precursors.

5.1.1.1. Radioautography in the Testis

Formerly, Clermont (1963) demonstrated that several stages of development of the spermatogonia were found at different levels in the germinal epithelium of mature man and rodents, with the most primitive germ cells found at the base and the more

differentiated cells located at higher levels by means of ^{3}H-thymidine radioautography. We studied the DNA, RNA and protein syntheses in aging mouse testis by LM and EM radioautography, demonstrating the incorporations of ^{3}H-thymidine, ^{3}H-uridine and ^{3}H-leucine into various cells of the seminiferous tubules (Gao, 1993; Gao *et al.*, 1994; Nagata *et al.*, 2000b; Nagata, 2002). DNA synthesis of spermatogenic cells was weak and only a few labeled spermatogonia could be observed during the embryonic stage (Fig. 11A). The labeled spermatogonia were also recognized at neonatal stages on postnatal day 4 and 7 (Fig. 11B) and the number of labeled spermatogonia increased from 2 weeks after birth, keeping high levels from 1 month (Fig. 11C) to 1 year (Fig. 11D) and even at 2 years (Gao, 1993). The labeling index of spermatogonia first peaked at 3 weeks and stayed constant until senescence at 1 and 2 years (Fig. 12A). However, the myoid cells and Sertoli's cells labeled with ^{3}H-thymidine were frequently observed at perinatal stages from embryo (Fig. 11A) to postnatal day 7 (Fig. 11B), while the labeling indices of both cells decreased from juvenile stage at postnatal 2 weeks to adult and senescence stages (Fig. 12B, 12C). On the other hand, the RNA synthesis (Fig. 11E,11F) and protein synthesis (Fig. 11G,11H) of various cells in the seminiferous tubules were studied using ^{3}H-uridine and ^{3}H-leucine incorporations (Gao *et al.*, 1994; Nagata, 2002a). The number of silver grains in both nuclei and cytoplasm of spermatogenic cells, Sertoli cells and myogenic cells showing RNA synthesis increased from perinatal stage (Fig. 11E) to adult and senescent stages (Fig. 11F). The number of silver grains in both nuclei and cytoplasm of spermatogenic cells, Sertoli cells and myogenic cells showing protein synthesis also increased from perinatal stage (Fig. 11G) to adult and senescent stages (Fig. 11H). The synthetic activities of RNA and proteins as shown by grain counting with ^{3}H-uridine (Fig. 13) and ^{3}H-leucine (Fig. 14) were weak at the embryonic and neonatal stages but increased at adult stage and maintained high levels until senescence (Gao *et al.*, 1994). These results showed that DNA synthesis in Sertoli cells and myoid cells increased at the perinatal stages and decreased from postnatal 2 weeks, while the DNA synthesis in spermatogonia increased from postnatal 2 weeks to senescence along with RNA and protein syntheses.

The Leydig cells or the interstitial cells of the testis are endocrine cells secreting steroid hormone, such as testosterone. They are located in the spaces between the seminiferous tubules and are identified as spherical, oval, or irregular cells in shape presenting central nuclei and numerous lipid droplets in the cytoplasm (Fig. 15). We studied the macromolecular synthesis of the cells in the testis of several groups of litter ddY mice at various ages from fetal to senescence by LM and EM RAG, using ^{3}H-thymidine, ^{3}H-uridine and ^{3}H-leucine incorporations (Gao *et al.*, 1995a,b; Nagata *et al.*, 2000b). Some of the Leydig cells from perinatal stage (Fig. 15A) to senescent stage (Fig. 15B) were labeled with ^{3}H-thymidine as observed by LMRAG. Changes in number of labeled Leydig cells showing DNA synthesis were found after the ^{3}H-thymidine incorporation into the nuclei of these cells in different aging groups. Only a few cells were labeled after ^{3}H-thymidine at embryonic day 19. At early postnatal stages, immediately after birth, there was a slight

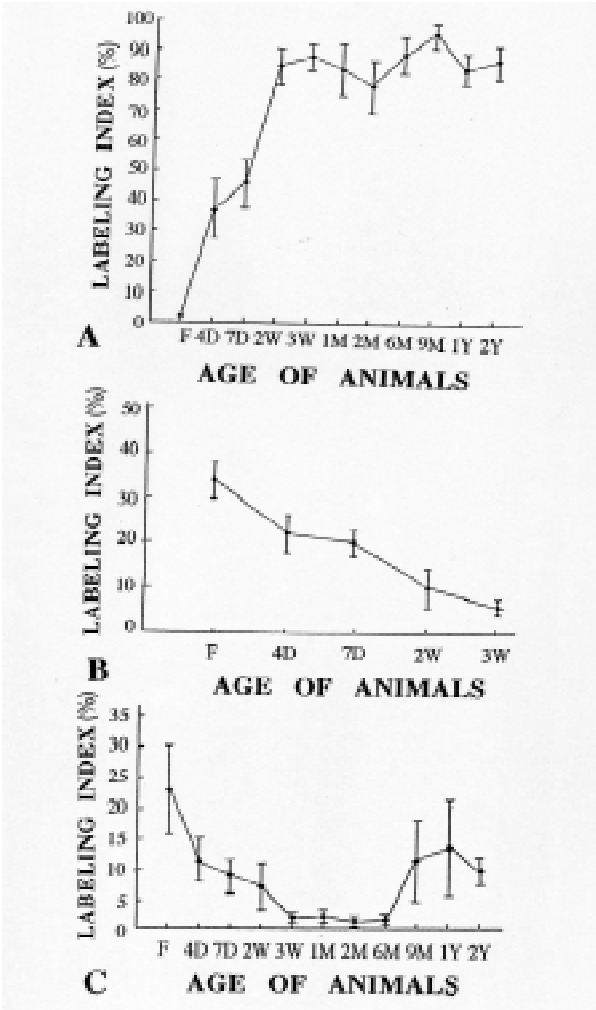

Fig. 12. Transitional curves of the labeling indices of the cells in the testis of aging mice at different ages from embryo to postnatal 2 years, labeled with ^{3}H-thymidine *in vitro*, showing DNA synthesis. The relationship between the labeling indices (ordinate) and the aging (abscissa). Mean ± standard deviation. From Gao (1993). **(A)** The labeling indices of the spermatogonia; **(B)** The labeling indices of the Sertoli cells; **(C)** The labeling indices of the myoid cells.

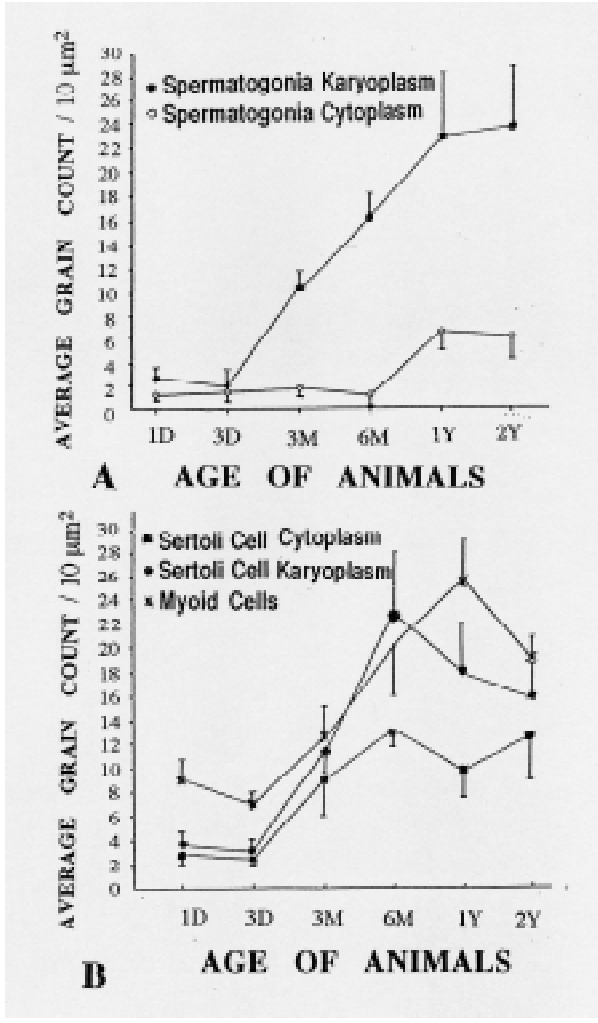

Fig. 13. Transitional curves of the grain counts of the cells (ordinate) in the testis of aging mice at different ages (abscissa) from newborn postnatal day 1 to senescent postnatal year 2, labeled with ^{3}H-uridine *in vitro* showing RNA synthesis. Mean ± standard deviation. From Gao (1993). **(A)** The grain counts of the spermatogonia; **(B)** The grain counts of the Sertoli cells and the myoid cells.

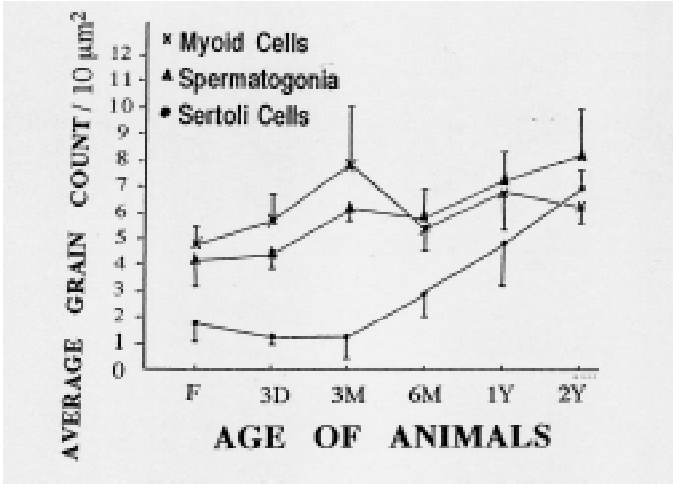

Fig. 14. Transitional curve of the grain counts (ordinate) of the cells in the testis of aging mice at different ages (abscissa) from embryo to postnatal year 2, labeled with ^{3}H-leucine *in vitro* showing protein synthesis. Mean ± standard deviation. From Gao (1993).

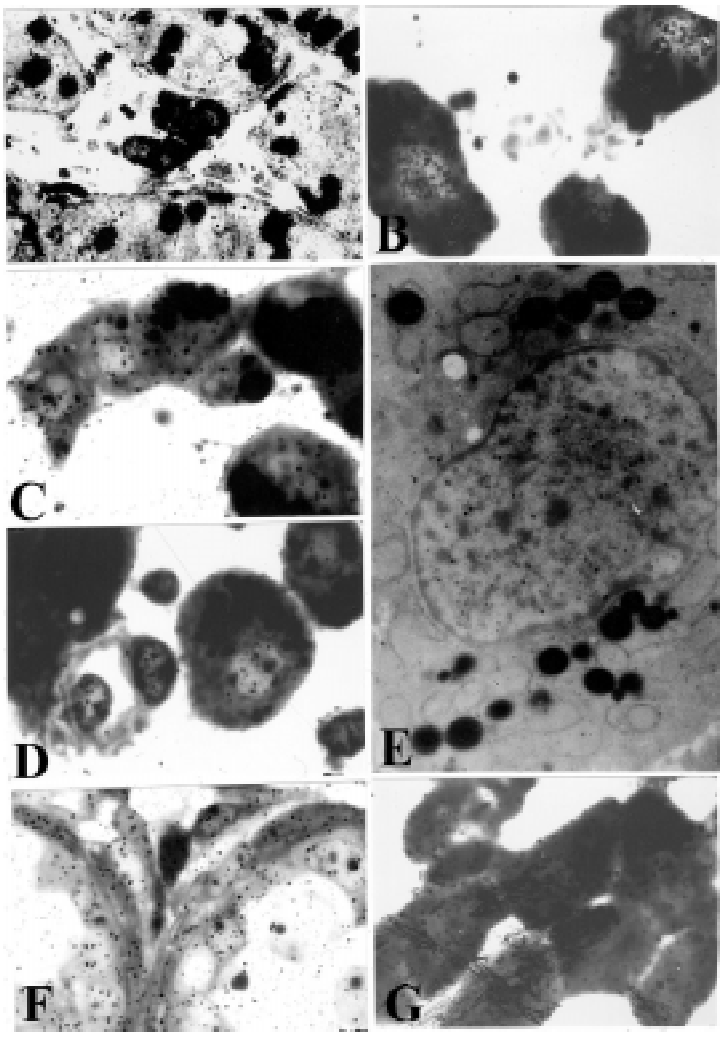

Fig. 15. Light and electron micrographs showing radioautographs of the interstitial cells of Leydig in the testis of mice. From Nagata *et al.* (2000b). **(A)** LMRAG of the testis of a perinatal mouse at postnatal day 1, labeled with ^{3}H-thymidine *in vitro*, showing the interstitial tissues at the center, surrounded by 4 seminiferous tubules. Note that several nuclei of Leydig cells are covered with silver grains demonstrating DNA synthesis at the center in this photograph. x300; **(B)** LMRAG of the interstitial tissue of the testis of a senescent mouse at postnatal month 12, labeled with ^{3}H-thymidine in vitro, demonstrating DNA synthesis in the 2 nuclei of two Leydig cells among 3 cells in this photograph. x1,000; **(C)** LMRAG of the interstitial tissue of the testis of a newborn mouse at postnatal day 3, labeled with ^{3}H-uridine *in vitro*, demonstrating RNA synthesis. Many sliver grains can be seen over all the nuclei and cytoplasm of all Leydig cells. x1,000; **(D)** LMRAG of the interstitial tissue of the testis of a newborn mouse at postnatal 1 month, labeled with ^{3}H-uridine *in vitro*, demonstrating RNA synthesis. Many sliver grains can be seen over all the nuclei and cytoplasm of all Leydig cells. x1,000; **(E)** EMRAG of a Leydig cell of a senescent mouse at postnatal month 12, labeled with ^{3}H-uridine *in vitro*, demonstrating RNA synthesis. Many sliver grains can be seen over all the nuclei and cytoplasm of all Leydig cells. Many sliver grains can be seen over the chromatin in the nucleus and abundant cell organelles such as endoplasmic reticulum and mitochondria in the cytoplasm, but no silver grains over lipid droplets. x8,000; **(F)** LMRAG of the testis of a mouse at embryonic day 19, labeled with ^{3}H-leucine, demonstrating protein synthesis. Many sliver grains can be seen over all the nuclei and cytoplasm of all Leydig cells at the center top as well as the spermatogonia and Sertoli cells in the seminiferous tubules surrounding the interstitial tissue. x500; **(G)** LMRAG of the testis of a senescent mouse at postnatal month 12, labeled with ^{3}H-leucine, demonstrating protein synthesis. Less sliver grains can be seen over all the nuclei and cytoplasm of all Leydig cells. x1,000.

increase of the number of labeled cells (Fig. 15A). The number of labeled cells from perinatal stage to postnatal 14 days and 1, 2, 6 months were similar to the values found at prenatal and early postnatal stages. The notable increases in the number of labeled Leydig cells were found from 9 months to 2 years in senescence (Fig. 15B). The labeling indices with ^{3}H-thymidine in perinatal stages to postnatal 6 months were low (5-10%) but increased at 9 months and maintained high level (50-60%) to 2 years (Gao *et al.*,1995b; Nagata *et al.*, 2000b). The labeling indices at senescent stages still maintained a relatively high level and they were obviously higher than those of young animals (Fig. 16A). The incorporation of ^{3}H-uridine into RNA was observed in almost all the Leydig cells in the interstitial tissues of the testis from embryonic day 19 until 2 years after birth (Gao *et al.* 1995a; Nagata *et al.* 2000b). A few silver grains over the nuclei and cytoplasm of Leydig cells labeled with ^{3}H-uridine were observed at embryonic day 19. The silver grains over those cells slightly decreased at postnatal day 1, 3 (Fig. 15C) and 7. The number of the silver grains over the nuclei increased from postnatal 1 month (Fig. 15D) to 6 months, 1 and 2 years (Fig. 15E). The average number of silver grains over the cytoplasm increased gradually and reached the maximum at 12 months after birth (Fig. 16B). At each stage, silver grains were mainly localized over the euchromatins and nucleoli in the nuclei of Leydig cells as observed by EMRAG (Fig. 15D). By electron microscopy, Leydig cells contained abundant cell organelles such as smooth surfaced endoplasmic reticulum, Golgi apparatus, mitochondria and lipid droplets (Fig. 15E). From adult to senescent stages, the activity of RNA synthesis maintained a high level in their nuclei as compared to the cytoplasm. In the cytoplasm of Leydig cells in respective aging groups some of the mitochondria and endoplasmic reticulum were also labeled with silver grains. It is noteworthy of notice that the average grain counts increased prominently in the senescent aging groups at 1 and 2 years after birth (Fig. 16B).

The incorporation of ^{3}H-leucine into proteins was also observed in almost all Leydig cells in the interstitial tissues of the testis by LM and EMRAG. The silver grains were located over the nuclei and cytoplasm of respective Leydig cells from perinatal stage (Fig. 15F) to senescence (Fig. 15G). The aging change of protein synthesis of Leydig cells among different aging groups was also found (Gao *et al.* 1995a; Nagata *et al.* 2000a). At embryonic day 19, the silver grains of Leydig cells labeled with ^{3}H-leucine was observed in both nucleus and cytoplasm and there was no obvious difference between the number of silver grains on the cytoplasm and the nucleus. The number of silver grains decreased at postnatal day 1 and then increased at day 3 and 7. However, the number of silver grains on both the nucleus and cytoplasm decreased from 1 month to 3 months and increased again from 6 months onwards maintaining a high level from adult to senescent stages (Fig. 17). Some of the silver grains were also localized over some of the mitochondria in respective aging groups as observed by EMRAG. These results indicate that the DNA, RNA and protein syntheses in Leydig cells were maintained at rather high level even at senescent stages at postnatal 1 and 2 years (Gao *et al.* 1995a; Nagata *et al.* 2000a).

5.1.1.2. X-ray Microanalysis in the Testis

A few papers are available in the literature treating X-ray microanalysis of some elements such as lead in the testis of male genital organ of experimental animals.

5.1.1.2.1. Lead in the Testis

Over the period of the last 40 years there was a marked decrease in the number of spermatozoa produced by the gonads of men. It was supposed that this fact was due to the influence of environmental pollution, wherein the lead played an important role. In sperms of men, professionally exposed to lead compounds, oligo-, asteno-, and teratospermia was disclosed. However, no literature is available dealing with the X-ray microanalysis of the testis obtained from such human patients. The localization of lead (Pb) in the testis of rats experimentally exposed to lead acetate was reported (Marchlewicz 1994). On the other hand, the localization of lead (Pb) in the testis of rats experimentally exposed to lead acetate was reported (Marchlewicz 1994). Studies were performed on sexually mature male rats after 9-month-long exposure to lead acetate as well as a group of animals after 3-month-long interval in the exposure. The changes provoked by the lead were evaluated by employing a number of study techniques, namely: 1) morphological examination of testes with taking into account the stages of seminiferous epithelial cycle, and epididymis, giving due consideration to zones; 2) electron microscopic examination of seminiferous cells and interstitial tissue, as well as the cells in the wall of epididymis and spermatozoa; 3) XMA determining the presence and type of elements on ultrathin section; 4) spectrophotometrical determination of Pb content in blood, testes and epididymides; 5) determination of testosterone concentration in blood serum. It has been revealed that the blood-testis barrier protects seminiferous epithelium against the toxic action of the lead. No deposits of Pb were observed either in germinal cells or Sertoli cells. The endocrine testicular cells outside the barrier had also unchanged ultrastructure and contained no Pb. That finding was expressed by normal testosterone level in blood serum. The only cells in the area of the testis, in whose cytoplasm there was Pb confirmed by XMA, were macrophages in the interstitial tissue of the testis. Apart from that, it has been disclosed that the blood-epididymis barrier does not provide a barrier against this element. Pb deposits were seen in smooth myocytes, epithelial cells and in the lumen of epididymal duct. That correlated with a marked decrease in the number of epididymal spermatozoa and numerous damages involving their ultrastructure. It has been shown that the lead, when passing to the duct lumen of epididymis through cells and structures constructing the wall of that organ, is being excreted from the male genital system with the sperm.

5.1.2. Auxiliary Glands

A few papers are available in the literature treating X-ray microanalysis of some elements such as zinc and magnesium in the auxiliary glands of male genital organs

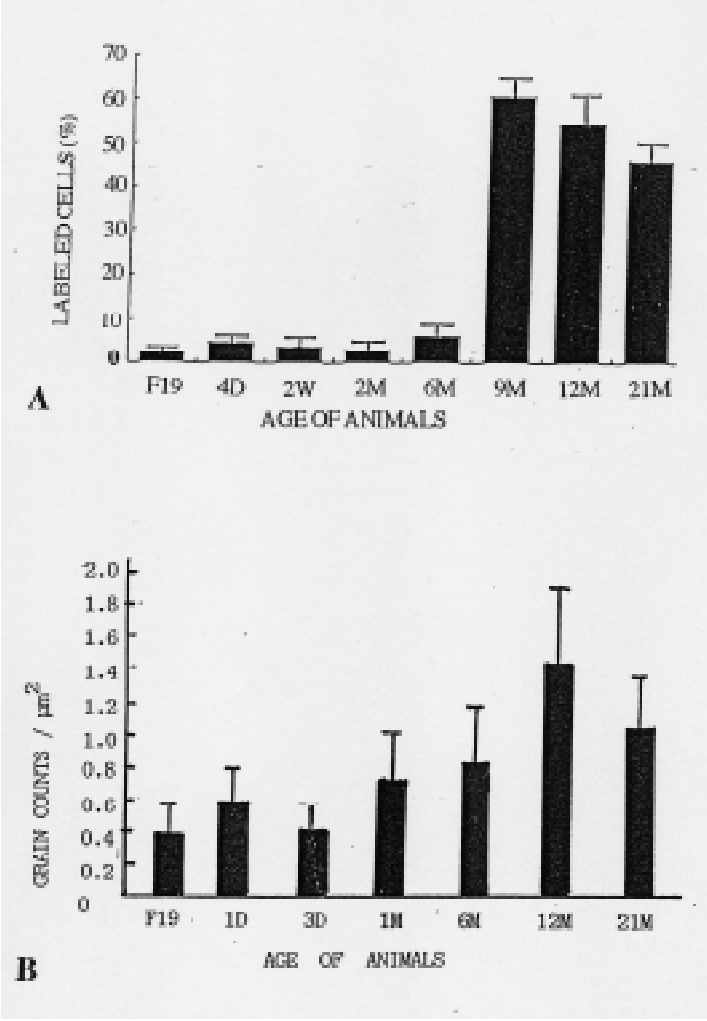

Fig. 16. Histograms showing transitional changes of the nucleic acid synthesis in Leydig cells of the testis of male mice at various ages. From Nagata *et al.* (2000b). **(A)** Relationship between the labeling indices with ^{3}H-thymidine indicating DNA synthesis (ordinate) and the aging (abscissa); **(B)** Relationship between the silver grain counts labeled with ^{3}H-uridine indicating RNA synthesis (ordinate) and the aging (abscissa). Mean ± standard deviation.

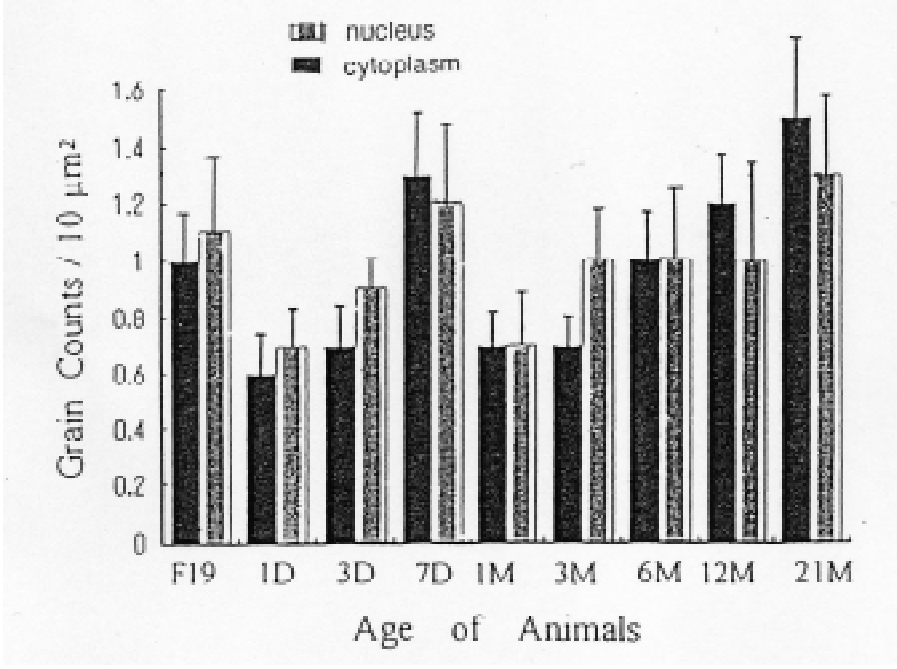

Fig. 17. Histograms showing transitional changes of the silver grain counts (ordinate) labeled with ^{3}H-leucine indicating protein synthesis in Leydig cells of the testis of male mice at various ages due to aging (abscissa). Mean ± standard deviation. From Nagata *et al.* (2000b).

of men and experimental animals.

5.1.2.1. X-ray Microanalysis in the Auxiliary Glands

In the literature, only a few papers on zinc (Zn) in the prostate glands of human patients as well as on magnesium (Mg) and sulfur (S) in the bulbourethral glands of rats are available by means of X-ray microanalysis (XMA).

5.1.2.1.1. Zinc in the Prostate Gland

Zinc (Zn) was detected in both normal and pathological prostate glands of men suffering from the prostatic diseases by XMA (Bataineh *et al.*, 2002). From the results, Zn was demonstrated to localize in the normal and pathological prostate glands of human adults.

5.1.2.1.2. Magnesium in the Bulbourethral Gland

The advantages of cryo-fixation followed by cryo-sectioning and freeze-drying or embedding in epoxy resin after freeze-substitution or freeze-drying for examining electrolytes by XMA were formerly studied and discussed by many authors in various kinds of organs and tissues (Nagata, 2000b; 2004b,c). The method was applied to localize some electrolytes such as magnesium (Mg) in the mucous granules of the bulbourethral glands of adult rats (Takaya and Masuda, 1991). Magnesium was found to be one of the normal constituents of the bulbourethral glands of normal adult rats.

5.1.2.1.3. Sulfur in the Bulbourethral Gland

The cryo-fixation followed by cryo-sectioning and freeze-drying was also applied to localize some electrolytes by XMA. Takaya & Masuda (1991) studied the localization of sulfur (S) in the mucous granules of the bulbourethral glands of normal adult rats and clarified that S was one of the normal constituents of the bulbourethral glands of normal adult rats.

5.2. Female Reproductive System

The female reproductive system (or the female genital organ) consists of the ovary, the oviduct, the uterus, the vagina and the external genitalia. We have studied the macromolecular synthesis in the ovary, oviduct and uterus of several litters of aging and pregnant ddY mice by radioautography and cytochemistry.

5.2.1. Ovary

The ovaries of mammals are paired oval organs consisting of medullary region and cortical region where ovarian follicles develop. We studied chemical reactions in hamster ovary cells in vitro and radioautography and immunocytochemistry in the ovaries of several groups of mice in aging.

5.2.2.1. Chemical Reactions in the Ovary

As for the chemical reactions, we used an established cell line, CHO-K1 cells, obtained from the Chinese hamster ovary cells for in vitro experiments (Nagata, 1995c, 1997b, 1999a, 2000a,d). The CHO-K1 cells were trypsinized, suspended in Ham's F12 medium (Nissui, Tokyo, Japan) supplemented with 10% newborn bovine serum (Flow Laboratories, Stanmore, NSW, Australia) and seeded on formval coated gold meshes in plastic Petri dishes (Falcon Plastic, USA), and incubated in a CO2 incubator at 37°C for several days. For the experimental pinocytosis, the cells were cultured in a medium containing horse radish peroxidase (HRP), 1mg/ml medium, for 24, 48 hrs to induce pinocytosis. The cells were fixed in 2.5% glutaraldehyde solution, stained with DAB reaction (Angermüller & Fahimi, 1981), dehydrated in a critical point dryer (Hitachi HCP-1) and observed by high voltage electron microscopy using either JEOL JEM-4000EX or Hitachi H-1250M, taking stereo-pair pictures. The stereo-pair pictures were observed with stereoscopes or anaglyph type color pictures were composed from red and green pictures from both sides. When these CHO-K1 cells were observed after culture with a medium containing HRP for 24 and 48 hrs, the cells incorporated HRP particles into their cytoplasm by pinocytosis and many DAB positive vesicles throughout their cytoplasm from 24 to 48 hrs. The relative relationship between the dense DAB positive pinocytotic vesicles and the other less dense cell organelles such as mitochondria and endoplasmic reticulum were observed 3-dimensionally (Nagata, 1999a, 2000a,e, 2001a,b).

5.2.1.2. Radioautography in the Ovary

With regards to the physical methods in the ovary, we studied DNA and RNA syntheses in the developing virgin mice, 6 litters of 36 female mice at various ages from postnatal day 1 to 60, by ^{3}H-thymidine and ^{3}H-uridine radioautography. The ^{3}H-thymidine incorporations were active in some of the nuclei in the surface epithelial cells, the stromal cells and the follicular cells of the ovary between postnatal day 1 (Fig. 18A) to 7 but decreased from day 14 (Fig. 18B) and maintained a lower level to day 60 (Li, 1994; Li & Nagata, 1995). The labeling indices with ^{3}H-thymidine incorporations were high at postnatal day 1 in all the surface epithelial cells, the follicular cells and the stromal cells and decreased from day 3 to 60 (Fig. 19A). The silver grains showing RNA synthesis labeled with ^{3}H-uridine incorporations were observed over all the nuclei and cytoplasm of all the cells in the surface epithelial cells, the follicular cells and the stromal cells of the ovary between postnatal day 1 (Fig. 18E) to 7 and maintained medium levels from day 14 on. The grain counts showing RNA synthesis were high at postnatal day from 1 to 7 and maintained medium levels at mature stage from day 14 to 60 (Fig. 20A). On the other hand, the mucosubstance synthesis with radiosulfate, 35SO4, was studied in the ovaries of female adult virgin mice during the estrus cycle (Li *et al.*, 1992). Four groups of female ddY mice, aged 8-10 weeks, were divided into 4 groups, diestrus, proestrus, estrus and metaestrus

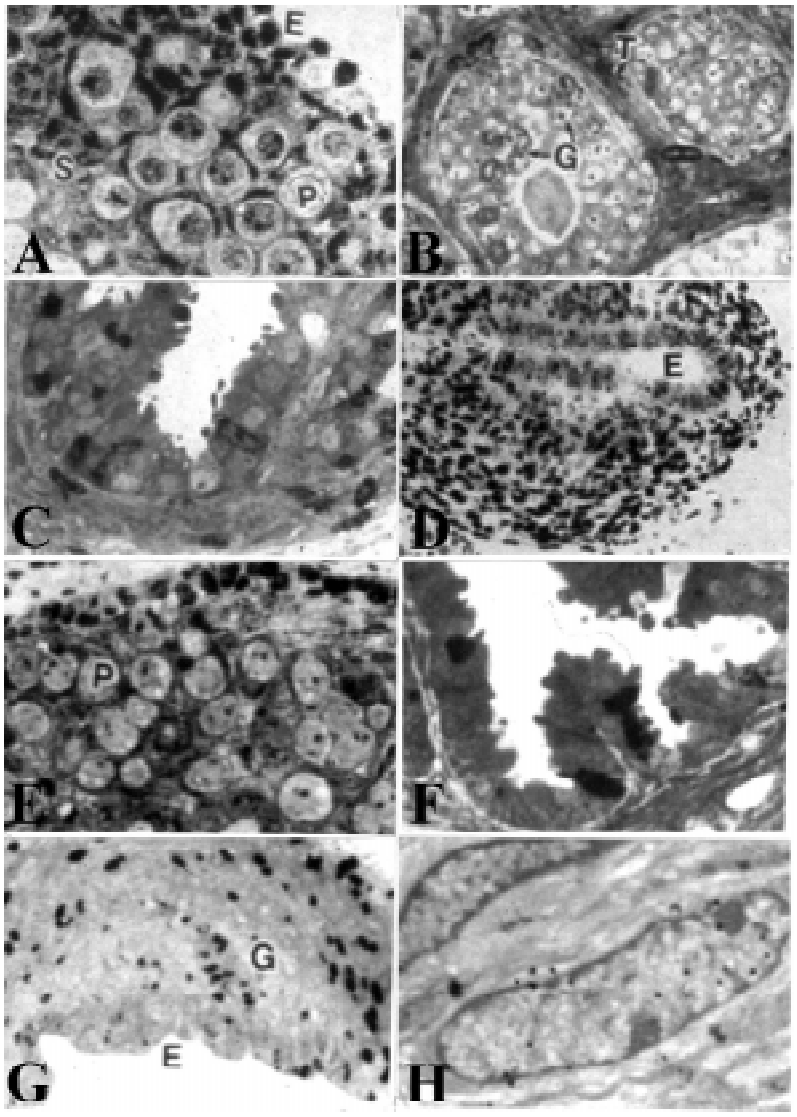

Fig. 18. Light and electron micrographs showing radioautographs of the female genital organs of mice. From Li & Nagata (1995). **(A)** LMRAG of the ovary of a female mouse at postnatal day 1, labeled with ^{3}H-thymidine in vitro. Many silver grains can be seen over the nuclei in surface epithelium (E), stroma (S) and the primordial follicles (P) showing DNA synthesis. x400; **(B)** LMRAG of the ovary of a female mouse at postnatal day 14, labeled with ^{3}H-thymidine in vitro. The nuclei of the granulosa (G) and theca (T) cells are labeled with silver grains. x500; **(C)** LMRAG of the oviduct of a female mouse at postnatal day 30, labeled with ^{3}H-thymidine in vitro. Several nuclei in the epithelial cells are labeled. x 500; **(D)** LMRAG of the uterus of a female mouse at postnatal day 1, labeled with ^{3}H-thymidine in vitro. Many nuclei in the epithelial cells (E) as well as most nuclei in the undifferentiated mesenchymal cells are labeled with silver grains showing DNA synthesis. x 500.

18E. LMRAG of the ovary of a female mouse at postnatal day 1, labeled with ^{3}H-uridine in vitro. Many silver grains are observed over the nuclei and cytoplasm of surface epithelium and primordial follicles (P) showing RNA synthesis. x 400; **(F)** LMRAG of the oviduct of a female mouse at postnatal day 30, labeled with ^{3}H-uridine in vitro. Many silver grains are observed over the nuclei and cytoplasm of the epithelial cells and smooth muscle cells. x 400; **(G)** LMRAG of the uterus of a female mouse at postnatal day 7, labeled with ^{3}H-uridine in vitro. Many silver grains are observed over the nuclei and cytoplasm of the epithelial cells (E) and smooth muscle cells and uterine glands (G). x 400; **(H)** EMRAG of the oviduct of a female mouse at postnatal day 30, labeled with ^{3}H-uridine in vitro. Several silver grains are observed over the nuclei and cytoplasm of the smooth muscle cells. x25,000.

according to the vaginal smears. The ovaries were taken out, labeled with 35SO4 in vitro and radioautographed. In all the animals, silver grains were localized over the granulosa and theca cells. Almost all compartments of the ovaries were labeled. The grain counts per cell changed according to cell cycle. The results showed that all the epithelial cells incorporated radiosulfate throughout the estrus cycle. Among the epithelial cells, much uptake was observed in granulosa and theca cells of the ovarian follicles. However, the number of silver grains decreased in the corpus luteum. These results revealed that the mucosubstance synthesis incorporating radiosulfate changed during the estrus cycle From the results, it is concluded that all the cells of the ovaries incorporated mucosubstances throughout the estrus cycle (Li *et al.*, 1992).

5.2.1.3. X-ray Microanalysis in the Ovary

We have not carried out any study on X-ray microanalsysis (XMA) in the ovary yet. In the literature, however, an article reporting the localizations of calcium (Ca) and cadmium (Cd) in the vitellogenic follicles of the ovary of *Galleria mellonella* as observed by XMA is available (Przelecka & Mrozinska, 2002). The results revealed the relation between the calcium-cadmium competition in the ovarian vitellogenic follicles.

5.2.1.4. Immunocytochemistry in the Ovary

With regards the biological reaction, we studied proliferating cell nuclear antigen (PCNA/cyclin) immunostaining in the ovary. It was demonstrated that PCNA/cyclin positive cells were observed in the ovarian surface epithelial cells, follicular cells and stromal cells (Li, 1994). The numbers of the PCNA positive cells were high on the postnatal day 1 to 3 and decreased from day 7 to 60. These results accorded well with the results obtained from the ^{3}H-thymidine radioautography (Li, 1994, Li & Nagata, 1995).

5.2.2. Oviduct

The oviduct or uterine tube is the first part of the female reproductive tract, a muscular tube, composed of 3 layers, mucosa, muscularis and serosa. We studied both radioautography and immunocytochemistry in the ovaries of several groups of mice in aging.

5.2.2.1. Radioautography in the Oviduct

We studied the DNA and RNA syntheses in the oviducts of developing virgin mice at various ages by ^{3}H-thymidine and ^{3}H-uridine radioautography (Li, 1994; Li & Nagata, 1995). The silver grains showing DNA synthesis were observed over many nuclei in the mucous epithelial cells, stromal and smooth muscle cells between postnatal days 1 to 3 and the number of labeled nuclei decreased from day 7 to 60 (Fig. 18C). The labeling indices with ^{3}H-thymidine incorporations were high at postnatal day 1 in the mucous epithelial cells and decreased gradually from day 3 to 60, while those in the stromal and

muscle cells increased from day 1 to day 3, reaching a peak, then decreased from day 7 to 60 (Fig. 19C). On the other hand, the silver grains showing RNA synthesis were observed over all the nuclei and cytoplasm of all the epithelial cells (Fig. 18F), stromal and muscle cells (Fig. 18H) from postnatal day 1 to 60. By grain counting, the number of silver grains in the epithelial cells increased from postnatal day 1 to day 7 then decreased from day 14 to day 60 (Fig. 20C), while the number of grains in the stromal and muscle cells increased from day 1 to day 3 and decreased from day 7 to 60 (Li & Nagata, 1995).

5.2.2.2. Immunocytochemistry in the Oviduct

With regards the biological reactions, we studied PCNA/cyclin immunostaining in the oviduct. It was demonstrated that PCNA/cyclin positive cells were observed in the tubal epithelial cells, tubal stromal and muscle cells (Li, 1994). The numbers of PCNA positive cells in the epithelial cells increased from postnatal day 1 to 14, then decreased from day 14 to 60, while the numbers in the stromal and muscle cells increased from day 1 to day 7 and decreased from day 14 to 60. These results accorded well with the results obtained from the ^{3}H-thymidine radioautography (Li, 1994, Li & Nagata, 1995).

5.2.3. Uterus

The uterus of mammals is a part of the female reproductive tract, an unpaired pear-shaped organ consisting of 3 layers, endometrium, myometrium and perimetrium. We studied both radioautography and immunocytochemistry in the uteri of several groups of female virgin mice in aging as well as in the uteri of adult mature mice during implantation.

5.2.3.1. Radioautography in the Uterus

We studied the DNA and RNA synthesis in the uteri of developing virgin mice at various ages by ^{3}H-thymidine and ^{3}H-uridine radioautography (Li, 1994; Li & Nagata, 1995). The silver grains showing DNA synthesis were observed over many nuclei in the endometrial epithelial cells and glandular cells, stromal and smooth muscle cells in the endometrial mucosa and myometrium (Fig. 18D) from postnatal days 1 to 3 and the number of labeled nuclei decreased from day 7 to 60. The labeling indices with ^{3}H-thymidine incorporations were high at postnatal day 1 and decreased gradually from day 3 to 60, in all the layers from the epithelial cells to the stromal and muscle cells (Fig. 19B). On the other hand, the silver grains showing RNA synthesis were observed over all the nuclei and cytoplasm of all the epithelial cells, stromal and muscle cells (Fig. 18G) from postnatal day 1 to 60. By grain counting, the number of silver grains in the epithelial cells increased from postnatal day 1 to day 7 then decreased from day 14 to day 60 (Fig. 20B), while the number of grains in the stromal and muscle cells increased from day 1 to day 3 and decreased from day 7 to 60 (Fig. 20B). These results showed that both DNA and RNA syntheses, as expressed by labeling indices and grain counting, were active in all kinds of cells, such as

endometrial epithelial cells, stromal cells and muscle cells of the uterus. However, the DNA synthesis in the epithelial cells and the stromal cells of both the uteri and the oviducts was active at postnatal day 1 and 3 and decreased from day 7 to 60, in contrast to the RNA synthesis in the uteri and oviducts which was low at postnatal day 1 and increased from day 1 to day 3, 7 and 14, and then decreased from day 30 to 60. Thus, the unparalleled alteration of the DNA and RNA syntheses was revealed between the ovary and the uterus or oviduct (Li and Nagata, 1995). The reason for this difference is not clear.

5.2.3.2. Immunocytochemistry in the Uterus

We studied PCNA/cyclin immunostaining in the uterus of several groups of aging ddY mice. It was demonstrated that PCNA/cyclin positive cells were observed in the endometrial epithelial cells, myometrial stromal and muscle cells (Li, 1994). The numbers of PCNA positive cells in the epithelial cells increased from postnatal day 1 to 7, then decreased from day 14 to 60, while the numbers in the stromal and muscle cells increased from day 1 to day 3 and decreased from day 7 to 60. These results accorded well with the results obtained from the ^{3}H-thymidine radioautography (Li, 1994, Li & Nagata, 1995).

5.2.4. Implantation

When an ovum of a mammal is fertilized in the oviduct, it moves towards the uterus forming the blastocyst and penetrates through the epithelium of the endometrium. This phenomenon is called as implantation. We studied the endometrium of pregnant mice after ovulations during the implantation window by radioautography, immunocytochemistry and lectin cytochemistry.

5.2.4.1. Radioautography in Implantation

In order to clarify the changes of DNA, RNA and protein synthesis during implantation, we studied the macromolecular synthesis in the uterus of the pregnant mouse by LM and EMRAG. It is well known that the uterus of the rodent becomes receptive to blastocyst implantation only for a restricted period. This is called the implantation window which is intercalated between refractory states of the endometrium whose cycling is regulated by ovarian hormones (Yoshinaga, 1988). We controlled the ovulations of mature female BALB/C strain mice during activation of the implantation in the mouse endometrium by administration of pregnant mare serum gonadotropin and human chorionic gonadotropin. Then, the pregnant female mice were ovariectomized on the 4th day of pregnancy. The delay implantation state was maintained for 48 hrs and after 0 to 18 hrs of estrogen supply, and ^{3}H-thymidine, ^{3}H-uridine and ^{3}H-leucine were injected into the mice, respectively. Then, we studied the changes of DNA (Yamada and Nagata, 1992a.b), RNA (Yamada and Nagata, 1993) and protein synthesis (Yamada, 1993) by ^{3}H-thymidine, ^{3}H-uridine and ^{3}H-leucine incorporations in the endometrial cells of pregnant-ovariectomized mice after time-lapse effect of nidatory estradiol. The three regions of the endometrium,

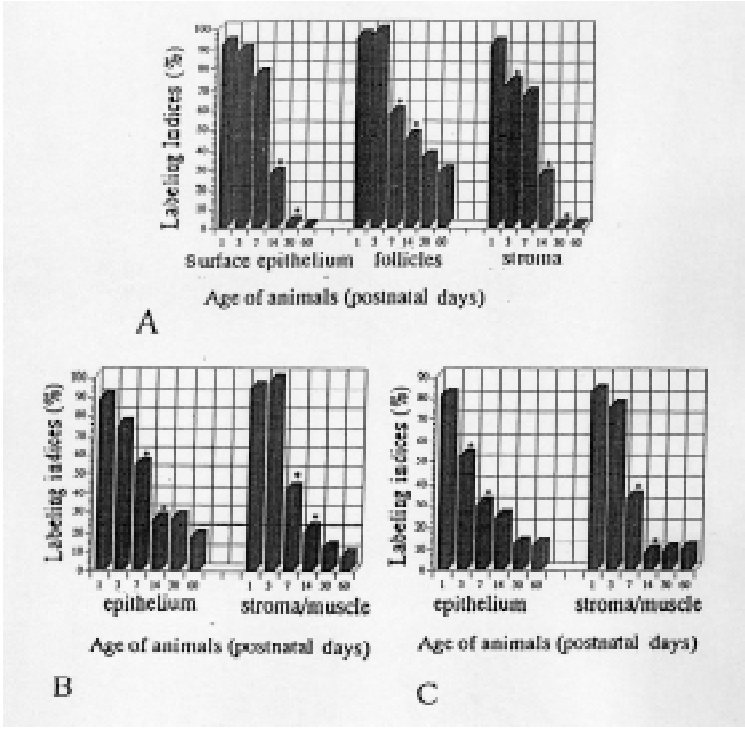

Fig. 19. Histograms showing the relationship between the labeling indices (ordinate) of mouse female genital cells, labeled with ^{3}H-thymidine and aging (abscissa) at various ages from postnatal day 1 to 60. From Li & Nagata (1995). **(A)** Labeling indices of ovary cells; **(B)** Labeling indices of uterine cells; **(C)** Labeling indices of tubal cells.

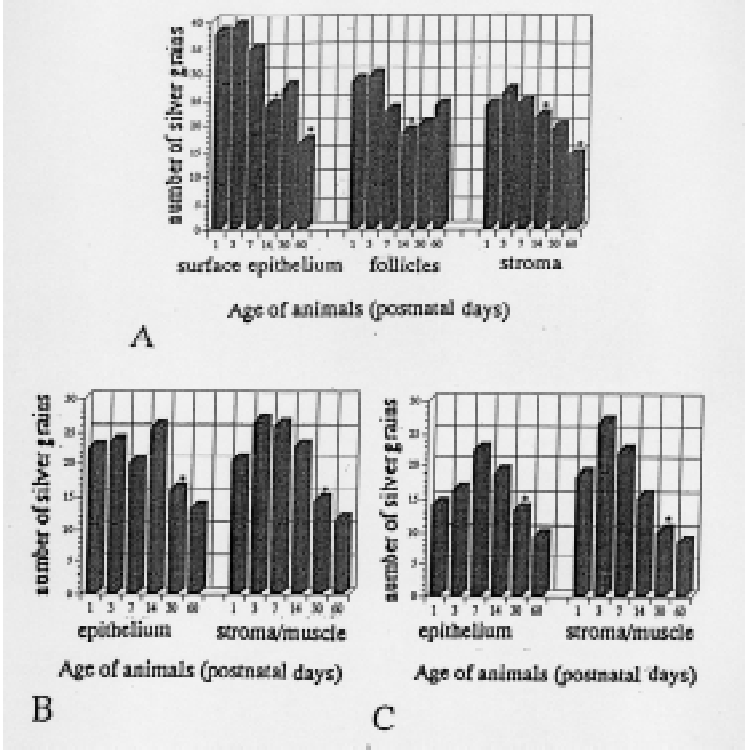

Fig. 20. Histograms showing the relationship between the average grain counts (ordinate) of mouse female genital cells, labeled with 3H-uridine and aging (abscissa) at various ages from postnatal day 1 to 60. From Li & Nagata (1995). **(A)** Grain counts of ovary cells; **(B)** Grain counts of uterine cells; (C) Grain counts of tubal cells.

i. e. the interimplantation site, the antimesometrial and mesometrial sides of implantation site, were taken out and processed for LM and EMRAG.. From the results, it was demonstrated that the endometrial cells showed topographical and chronological differences in the nucleic acid and protein synthesis. The cells labeled with ^{3}H-thymidine showing DNA synthesis increased after nidatory estradiol effects in the stromal cells around the blastocyst (Fig. 21A, 21B, 21D), but not in the epithelial cells (Fig. 21A, 21C). The cells labeled with ^{3}H-uridine showing RNA synthesis were observed in both epithelial cells (Fig. 21E) and stromal cells (Fig. 21F). The cells labeled with ^{3}H-uridine showing protein synthesis were also observed in both epithelial cells (Fig. 21G) and stromal cells (Fig. 21H). Quantitative analysis revealed that the labeling indices with ^{3}H-thymidine in the stromal cells at antimesometrial and mesometrial side of implantation sites and interimplantation sites increased from 0 hr to 3, 6, 12 and 18 hr, reaching a peak at 18 hrs after estrogen induction (Fig. 22). The number of silver grains as expressed by grain counting per mm2 in both the luminal epithelial cells (Fig. 23A) and the stromal cells (Fig. 23B) on the antimesometrial side labeled with ^{3}H-uridine showing RNA synthesis increased from 0 hr to 3 and 6 hr, reaching a peak at 6 hr and decreased from 12 to 18 hr. Likewise, the number of silver grains as expressed by grain counting per mm2 in both the epithelial cells (Fig. 24A) and the stromal cells (Fig. 24B) on the antimesometrial side labeled with ^{3}H-leucine showing protein synthesis increased from 0 hr to 3 and 6 hr, reaching a peak at 6 hr and decreased from 12 to 18 hr. These results suggested that the presence of the blastocysts in the uterine lumen induced selective changes in the behavior of endometrial cells after nidatory estradiol effect showing the changes of DNA, RNA and protein syntheses. The coincident time peak of RNA and protein synthesis detected in the endometrial cells at the anti-mesometrial side of the implantation site, probably reflected the activation moment of the implantation window (Yamada, 1993; Yamada and Nagata, 1992a,b; 1993).

On the other hand, the protein synthesis in the decidual cells of pregnant mice uteri was compared to the endometrial cells of virgin mice uteri using ^{3}H-proline and ^{3}H-tryptophane incorporations (Oliveira *et al.* 1991, 1995). The results demonstrated that silver grains were localized over the endoplasmic reticulum and the Golgi apparatus of fibroblasts and accumulated over collagen fibrils in the extracellular matrix suggesting that the decidual cells produced collagen in the matrix. The results suggested that the decidual cells produced collagen into the matrix. The quantitative analysis showed that both incorporations in the decidual cells and the matrix increased in the pregnant mice than the endometrial cells in virgin mice (Oliveira *et al.* 1991, 1995).

5.2.5.2. Immunocytochemistry in Implantation

The implantation and development of blastocyst to embryo in the uterus demand complex sequences of cellular and molecular modifications in the uterus (Zorn *et al.*, 2004). During the pre-implantation period, various morphological and biochemical

events occur including macromolecular synthesis and degradation of extracellular matrix (ECM) molecules, recruitment of the immune competent cells and increasing vascular permeability. Moreover, preceding the implantation, a wave of cell proliferation occurs in the endometrium following redifferentiation of endometrial fibroblasts into decidual cells. These phenomena culminate in the formation of a new temporary uterine structure called decidua (Abrahamsohn and Zorn, 1993; Abrahamsohn *et al.*, 2002). Much information has been accumulated to support the essential role of the decidua in maintaining normal pregnancies and proper embryo development. Abrahamsohn *et al.* (2002) reported the remodel of the fibrillar and non-fibrillar components of the endometrium during decidualization in rodents and human, by degradation and synthesis of ECM molecules such as glycosaminoglycans and proteoglycans. The decidual cells can synthesize collagen which is incorporated into thick collagen fibrils present in the fully decidualized region of the mouse endometrium (Oliveira *et al.*, 1995). Moreover, ultrastructural cytochemistry showed the differences of the arrangement and distribution of proteoglycans network in the endometrium between the pregnant and not pregnant mice. Zorn & San Martin (2004) showed that some ECM molecules such as decorin was present in the endometrium exclusively before the embryo implantation, whereas biglycan was expressed after the embryo implantation and was related with the thick collagen fibrils but not with the thin fibrils by means of immunocytochemical method. On the other hand, versican increased along the pregnancy whereas hialuronan disappeared from the decidualized areas of the endometrium but was concentrated in the mesometrial decidua. Considering these results, it is concluded that morphological and molecular changes observed during the pre-implantation period, together with the redifferentiation of endometrial fibroblasts into decidual cells, comprise a new selective genetic program. This new program is characterized by sequential and coordinate down and up regulation of various proteoglycans and glycosaminoglycans in the uterus a well as by an unusual fibrilogenesis of collagen fibrils (Oliveira *et al.*, 1995; San Martin *et al.*, 2003a,b).

5.2.5.3. Lectin Cytochemistry in Implantation

It is well known that the natural killer lymphocytes are the dominant leukocyte in the human and rodent uteri. Paffaro Jr. *et al.* (2003) reported that one of the lectins Dolichos biflorus (DBA) which is specific for GalNAc (N-acetyl-D-galactosamine) is a useful tool to identify and localize the mouse uterine natural killer cells (uNK). This lectin cytochemistry showed that the immature precursor form of uNK migrated and differentiated transiently in the uterus of mouse only during pregnancy. The contribution of paracrine releasing of cytokines by uNK to the successful pregnancy was well demonstrated, but direct evidence of their predicted response related to natural immunity inducing miscarriage has not yet been shown. Yamada *et al.* (2004) used the surgical embryo damage (ED) to induce abnormal status of pregnancy, as model to evaluate the uNK cytolytic behavior. The pregnant mice on 9th gestational day were sacrificed at 10, 30, 60 and 120 min after

embryo damage (ED) and sham-operated animals were used as control. The evaluations were performed by cuprolinic blue and lectin cytochemistry at both light and electron microscopic levels, as well as anti-perforin and anti-cathepsin D immunocytochemistry, and TUNEL (terminal-deoxynucleotidyl-transferase-mediated deoxyuridine-triphosphate-biotin nick end labeling) method for apoptosis. In the uNK of normal pregnant mice the majority of secretory-lysosome type granules showed a fine reticular distribution of proteoglycans in the core (secretory compartment) by cuprolinic blue cytochemistry, while the glycoconjugates stained by DBA lectin were present both in the cap and core regions. The anti-cathepsin D immunocytochemistry showed specific labeling in the cap (lysosome compartment) of all granules, but intriguingly not all mature forms of uNK showed positive granules with anti-perforin. Such heterogeneity of the granules suggested the presence of functionally distinct sub-populations of uNK cells in the uterine maternal-foetal interface. The ED affected the uterus inducing the local hyperemia and after 20 min, a hemorrhagic area was seen in the locus where uNK cells concentrated. These phenomena propagated rapidly to the untouched embryo implantation sites. The uNK cells found in such hyperemic area showed disrupted granules with discontinuous membranes and their content became weakly stained by cuprolinic blue, as was the reactivity against DBA lectin and cathepsin D. This looseness affected more granules in most of uNK as the time-effects of ED increased and many cells showed empty vacuoles in the cytoplasm. However, any ultrastructural image showing granule exocytosis was not seen. The perforin labeling was continuously seen in some of uNK cells. Large numbers of TUNEL positive nuclei were found in the trophoblast cells after ED, but the nuclei of endometrium stromal cells were not positively stained (Yamada *et al.*, 2004).

6. Concluding Remarks

The radioautographic and cytochemical methods that we have developed in our laboratory to demonstrate chemical components of cells and tissues including elements and macromolecules at both light and electron microscopic levels during these 40 years are reviewed and the results obtained by the application of these methods to the urogenital system of experimental animals are summarized.

The radioautographic and cytochemical results from the urogenital organs, such as the kidney, the testis, the ovary, the oviduct and the uterus including the changes by implantation, revealed that the macromolecular synthesis and cytochemical stainings of respective organs changed in connection with the aging of animals as well as implantation.

It is concluded that these aging changes could answer to some questions on the biology of aging how we get old demonstrating the transitional qualitative and quantitative changes of the chemical constituents of respective organs due to the aging of animals.

Acknowledgments: The author is grateful to many collaborators, former

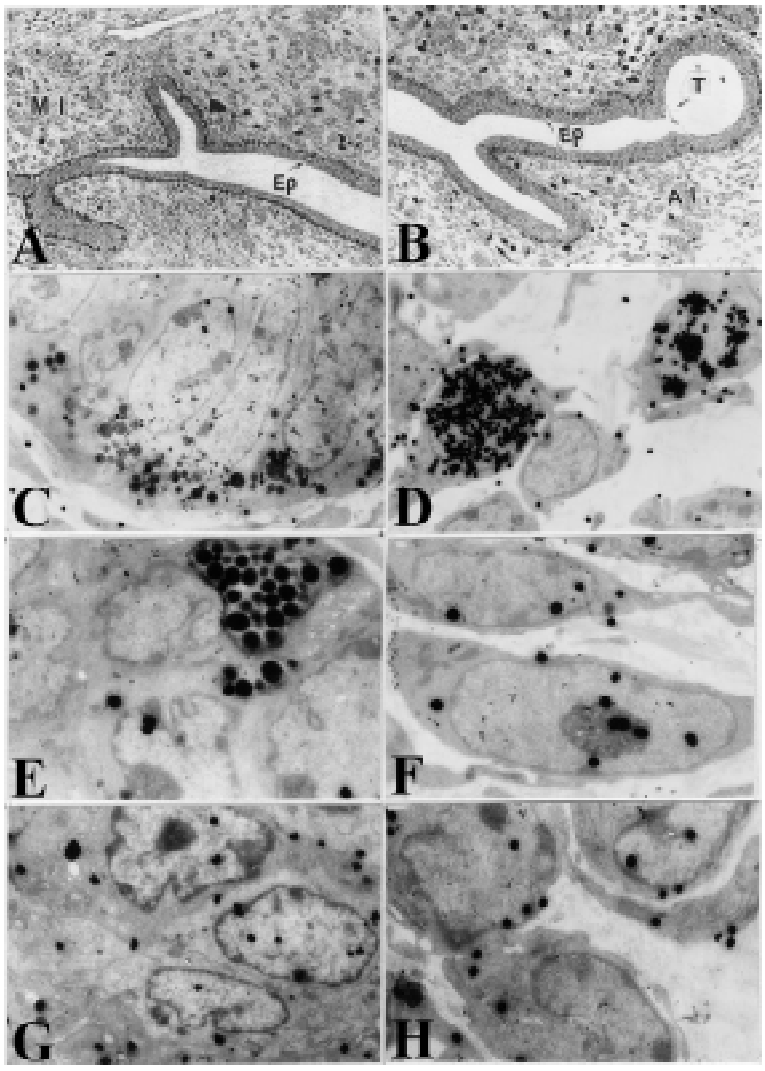

Fig. 21. Light and electron micrographs showing radioautographs of implantation. **(A)** LMRAG of the uterus of a pregnant-ovariectomized female mouse after estradiol treatment and labeled with ^{3}H-thymidine. Many stromal cells are labeled with silver grains demonstrating DNA synthesis at the mesometrial side of implantation (MI). No epithelial cell (Ep) is labeled. x200. Yamada & Nagata (1992). **(B)** LMRAG of the uterus of a pregnant-ovariectomized female mouse after estradiol treatment and labeled with 3H-thymidine. Many stromal cells are labeled demonstrating DNA synthesis at the antimesometrial side of implantation (AI). Trophoblast (T) is not labeled. x200. Yamada & Nagata (1992). **(C)** EMRAG of the epithelial cells of the uterus of a pregnant-ovariectomized female mouse after estradiol treatment and labeled with ^{3}H-thymidine. Two nuclei (at center) are labeled with silver grains. x3,000. Original picture; **(D)** EMRAG of the stromal cells of the uterus of a pregnant-ovariectomized mouse after estradiol treatment and labeled with ^{3}H-thymidine. Two stromal cells are labeled with silver grains. x3,000. Original picture; **(E)** EMRAG of the epithelial cells of the uterus of a pregnant-ovariectomized female mouse after estradiol treatment and labeled with 3H-uridine, demonstrating RNA synthesis. Four nuclei are labeled with silver grains. x 5,000. Original picture; **(F)** EMRAG of the stromal cells of the uterus of a pregnant-ovariectomized female mouse after estradiol treatment and labeled with ^{3}H-uridine. Two nuclei and nucleoli are labeled with silver grains, demonstrating RNA synthesis. x5,000. Original picture; **(G)** EMRAG of the epithelial cells of the uterus of a pregnant-ovariectomized female mouse after estradiol treatment and labeled with ^{3}H-leucine, demonstrating protein synthesis. Three nuclei are labeled with silver grains. x6,000. Original picture; **(H)** EMRAG of the stromal cells of the uterus of a pregnant-ovariectomized female mouse after estradiol treatment and labeled with ^{3}H-leucine. Three nuclei are labeled with silver grains, demonstrating protein synthesis. x6,000. Original picture.

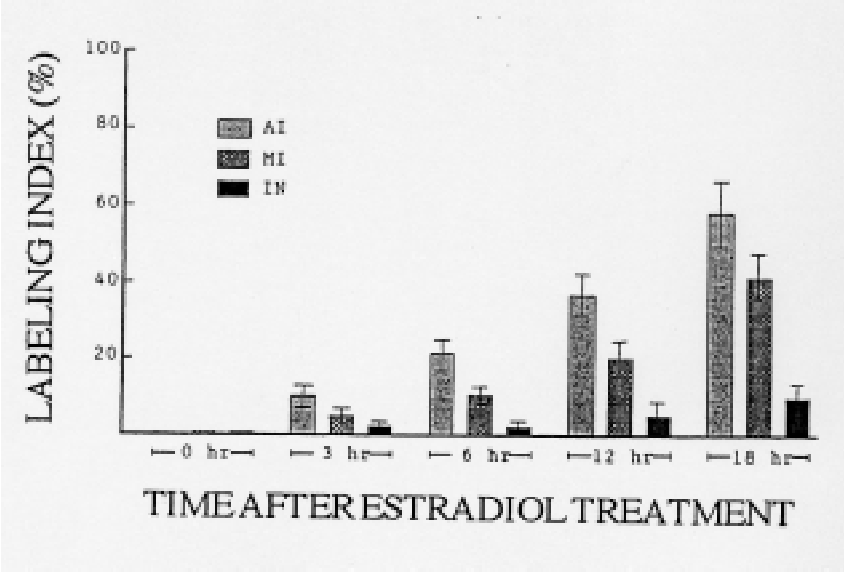

Fig. 22.Histogram showing labeling indices of stromal cells in respective sites, antimesometrial (AI), mesometrial (MI) side of implantation sites and interimplantation sites (IN), in the endometrium of the pregnant-ovariectomized female mice after estradiol treatment and labeled with 3H-thymidine indicating DNA synthesis. From Yamada and Nagata (1992).

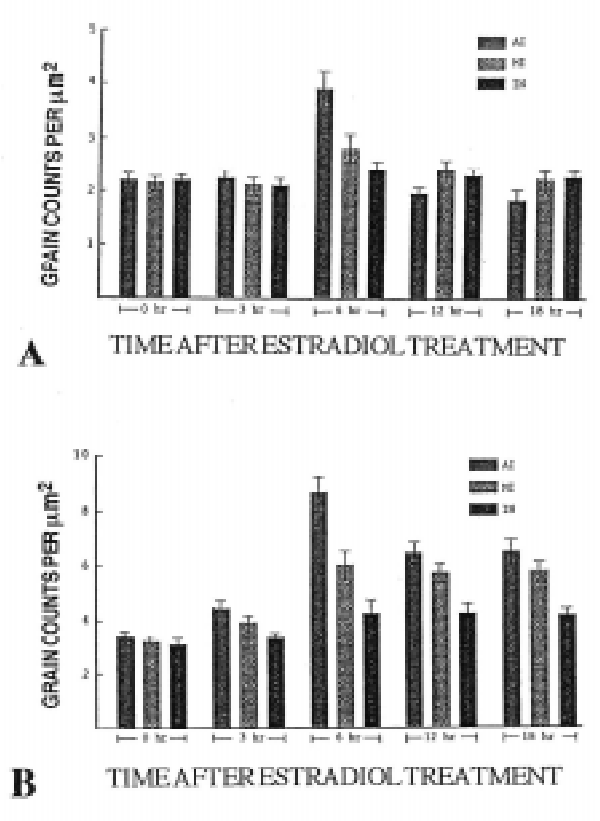

Fig. 23. Histogram showing grain counts (per square micrometer) incorporating 3H-uridine indicating RNA synthesis over the luminal epithelial cells (A) and stromal cells (B) of the pregnant-ovariectomized female mice after estradiol treatment. From Yamada and Nagata (1992).

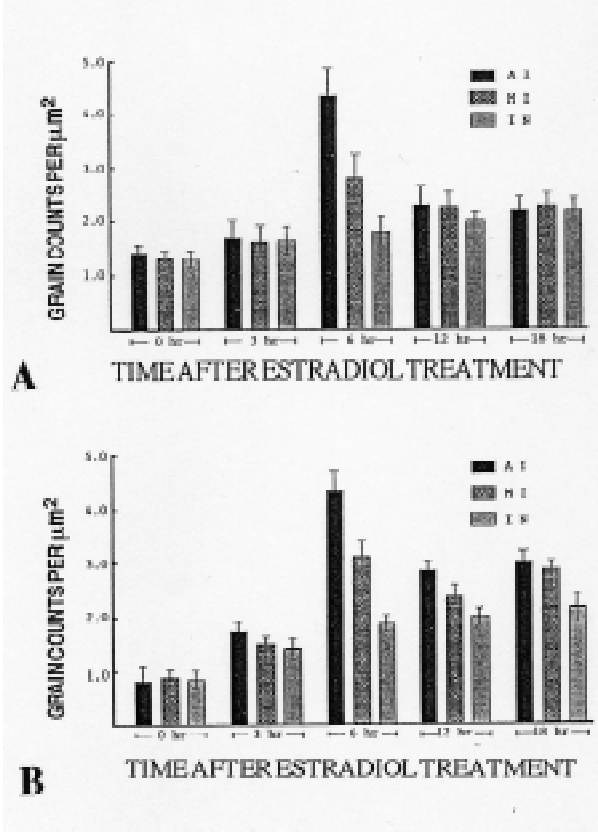

Fig. 24. Histogram showing grain counts (per square micrometer) incorporating ^{3}H-leucine indicating protein synthesis over the luminal epithelial cells (A) and stromal cells (B) of the pregnant-ovariectomized female mice after estradiol treatment. From Yamada and Nagata (1992).

graduate students, whose names are listed as the co-authored references including not only Japanese but also several foreign graduate students from Asian countries such as China, Indonesia, Philippines, as well as Brazil in South America. The author also thanks Dr. Kiyokazu Kametani, Technical Official, Department of Instrumental Analysis, Research Center for Human Environmental Sciences, Shinshu University, for his technical assistance during the course of these studies.

References

Abrahamsohn PA, Zorn TMT. Implantation and decidualization in rodents. J Exp Zool 1993;266:3-28.

Abrahamsohn PA, Zorn TMT, Oliveira. Decidua in rodents. In: Glasser S, Aplin J, Giudice L, Tabibzadeh S (eds.). The Endometrium. London: Taylor & Francis;2002:279-93.

Altmann R. Über die Fettumsetzungen im Organismus. Arch Anat Physiol 1889;Suppl:86-104.

Altmann R. Die Elementorganismen und ihre Beziehungen zu den Zellen. Leipzig: Veit und Comp, 1894.

Angermüller S, Fahimi HD. Selective cytochemical localization of peroxidase, cytochrome oxidase and catalase in rat liver with 3,3'-diamino-benzidine. Histochemistry 1981;71:33-44.

Bataineh ZM, Bani-Hani IH, Al-Alami JR. Zinc in normal and pathological human prostate gland. Saudi Med J 2002;23:218-20.

Caspersson T. Über die chemischen Aufbau des Struktur des Zellkernes. Skandinav Arch Physiol 1936;73(Suppl 8):1-151.

Chen S, Gao F, Kotani A, Nagata T. Age-related changes of male mouse submandibular gland: A morphometric and radioautographic study. Cell Mol Biol 1995;41:117-24.

Clermont Y. Renewal of spermatogonia in man. Amer J Anat 1963;112:35-51.

Commission on Enzymes of the International Union of Biochemistry: Report of the commission on enzymes of the international union of biochemistry. London: Pergamon Press; 1961.

Coons AH, Creech HJ, Jones RN. Immunological properties of an antibody containing a fluorescent group. Proc Exp Biol (NY) 1941;47:200-2.

Cui H. Light microscopic radioautographic study on DNA synthesis of nerve cells in the cerebella of aging mice. Cell Mol Biol 1995;41:1139-54.

Cui H, Gao F, Nagata T. Light microscopic radioautographic study on protein synthesis in perinatal mice corneas. Acta Histochem Cytochem 2000;33:31-7.

Duan H, Nagata T. Glomerular extracellular matrices and anionic sites in aging ddY mice: a morphometric study. Histochemistry 1993;99:81-91.

Duan H, Gao F, Li S, Hayashi K, Nagata T. Aging changes and fine structure and DNA synthesis of esophageal epithelium in neonatal, adult and old mice. J Clin Electron Microsc 1992;25:452-3.

Duan H, Gao F, Li S, Nagata T. Postnatal development of esophageal epithelium in mouse: a light and electron microscopic radioautographic study. Cell Mol Biol 1993;39:309-16.

Feulgen R, Rossenbeck H. Mikroskopisch-chemischer Nachweiss einen Nukleinsäure von Typus der Thymonukleinsäure. Z Physik Chem 1924;135:203-48.

Gao F. Study on the macromolecular synthesis in aging mouse seminiferous tubules by light and electron microscopic radioautography. Cell Mol Biol 1993;39:659-72.

Gao F, Toriyama K, Nagata T. Light microscopic radioautographic study on the DNA synthesis of prenatal and postnatal aging mouse retina after labeled thymidine injection. Cell Mol Biol 1992a;38:661-8.

Gao F, Li S, Duan H, Ma H, Nagata T. Electron microscopic radioautography on the DNA synthesis of prenatal and postnatal mice retina after labeled thymidine injection. J Clin Electron Microsc 1992b;25:721-2.

Gao F, Toriyama K, Ma H, Nagata T. Light microscopic radioautographic study on DNA synthesis in aging mice corneas. Cell Mol Biol 1993;39:435-41.

Gao F, Ma H, Sun L, Jin C, Nagata T. Electron microscopic radioautographic study on the nucleic acids and protein synthesis in the aging mouse testis. Med Electron Microsc 1994;27:360-2.

Gao F, Chen S, Sun L, Kang W, Wang Z, Nagata T. Radioautographic study of the macromolecular synthesis of Leydig cells in aging mice testis. Cell Mol Biol 1995a;41:145-50.

Gao F, Jin C, Ma H, Sun L, Nagata T. Ultrastructural and radioautographic studies on DNA synthesis in Leydig cells of aging mouse testis. Cell Mol Biol 1995b;41:151-60.

Gersh I. The Altmann technique for fixation by drying while freezing. Anat Rec 1932;53:309-24.

Gersh I. The preparation of frozen-dried tissues for electron microscopy. J Biophys Biochem Cytol 1956;2(Suppl):37-43.

Gomori G. Microtechnical demonstration of phosphatase in tissue sections. Proc Soc Exp Biol Med 1939;42:23-6.

Gunarso W, Gao F, Cui H, Ma H, Nagata T. A light and electron microscopic radioautographic study on RNA synthesis in the retina of chick embryo. Acta Histochem 1996;98:309-22.

Gunarso W, Gao, F, Nagata T. Development and DNA synthesis in the retina of chick embryo observed by light and electron microscopic radioautography. Cell Mol Biol 1997;43:189-201.

Hanai T. Light microscopic radioautographic study of DNA synthesis in the kidneys of aging mice. Cell Mol Biol 1993;39:81-91.

Hanai T, Nagata T. Study on the nucleic acid synthesis in the aging mouse kidney by light and electron microscopic radioautography. In: Nagata T. (ed.). Radioautography in Medicine, Matsumoto: Shinshu University Press; 1994a:209-14.

Hanai T, Nagata T. Electron microscopic study on nucleic acid synthesis in perinatal mouse kidney tissue. Med Electron Microscopy 1994b;27:355-7.

Hanai T, Usuda N, Morita T, Shimizu T, Nagata T. Proliferative activity in the kidneys of aging mice evaluated by PCNA/cyclin immunohistochemistry. Cell Mol Biol 1993;39:181-91.

Hanai T, Usuda N, Morita T, Nagata T. Light microscopic lectin histochemistry in aging mouse kidney: Study of compositional changes in glycoconjugates. J Histochem Cytochem 1994a;42:897-906.

Hanai T, Usuda N, Morita T, Nagata T. Correspondence to changes in lectin binding pattern during fetal and postnatal development of renal corpuscles of rat kidney as revealed by light and electron microscopy. Acta Histochem Cytochem 1994b;27:185-8.

Hanai T, Usuda N, Morita T, Nagata T. Light microscopic lectin histochemistry in aging mouse kidney: Study of compositional changes in glycoconjugates. J Histochem Cytochem 1994c;42:897-906.

Hanai T, Usuda N, Morita T, Nagata T. Changes in lectin binding pattern during fetal and postnatal development of renal corpuscles of the rat kidney as revealed by light and electron microscopy. Acta Histochem Cytochem 1994d;27:185-8.

Hayashi K, Gao F, Nagata T. Radioautographic study on ^{3}H-thymidine incorporation at different stages of muscle development in aging mice. Cell Mol Biol 1993;39:553-60.

Ito M. The radioautographic studies on aging change of DNA synthesis and the ultrastructural development of mouse adrenal gland. Cell Mol Biol 1996;42:279-92.

Ito M, Nagata T. Electron microscopic radioautographic studies on DNA synthesis and ultrastructure of aging mouse adrenal gland. Med Electron Microsc 1996;29:145-52.

Jin C. Study on DNA synthesis of aging mouse colon by light and electron microscopic radioautography. Cell Mol Biol 1996;42:255-68.

Jin C, Nagata T. Light microscopic radioautographic study on DNA synthesis in cecal epithelial cells of aging mice. J Histochem Cytochem 1995a;43:1223-8.

Jin C, Nagata T. Electron microscopic radioautographic study on DNA synthesis in cecal epithelial cells of aging mice. Med Electron Microscopy 1995b;28:71-5.

Johkura K. The aging changes of glycoconjugate synthesis in mouse kidney studied by ^{3}H-glucosamine radioautography. Acta Histochem Cytochem 1996;29:57-63.

Johkura K, Usuda N, Nagata T. Quantitative study on the aging change of glycoconjugates synthesis in aging mouse kidney. Proc Xth Internat Cong Histochem Cytochem, Kyoto, Acta Histochem Cytochem 1996; 29(Suppl):507-8.

Kametani K. Detection of aluminum by energy dispersive X-ray microanalysis at high accelerating voltages with semi-thin sections of biological sample. J Electron Microscopy 2002;51:265-74.

Kametani, K., Nagata, T.: Detection of small amount of Al element in tissues by EDX-HVEM and EELS-ESI. Proc. 8th APEM (Asia-Pacific Conference on Electron

Microscopy), Kanazawa; 2004: 1110-1.

Kametani K, Suzuki K, Nagata T. X-ray microanalysis at high accelerating voltage detecting aluminum accumulation in mouse kidney after short-term aluminum administration. Acta Histochem Cytochem 2003;36:221-30.

Kong Y. Electron microscopic radioautographic study on DNA synthesis in perinatal mouse retina. Cell Mol Biol 1993;39:55-64.

Kong Y, Nagata T. Electron microscopic radioautographic study on nucleic acid synthesis of perinatal mouse retina. Med Electron Microscopy 1994;27:366-8.

Kong Y, Usuda N, Nagata T. Radioautographic study on DNA synthesis of the retina and retinal pigment epithelium of developing mouse embryo. Cell Mol Biol 1992a;38:263-72.

Kong,Y, Usuda N, Morita T, Hanai T, Nagata T. Study on RNA synthesis in the retina and retinal pigment epithelium of mice by light microscopic radioautography. Cell Mol Biol 1992b;38:669-78.

Leblond C P. The life history of cells in renewing systems. Am J Anat 1981;160:113-58.

Li S. Relationship between cellular DNA synthesis, PCNA expression and sex steroid hormone receptor status in the developing mouse ovary, uterus and oviduct. Histochemistry 1994;102:405-13.

Li S, Duan H, Nagata T. Age-related alterations of proteoglycan in mouse tracheal cartilage matrix: An electron histochemical analysis with the cationic dye of polyethylenimine. Cell Mol Biol 1994;40:129-35.

Li S, Gao F, Duan H, Nagata T. Radioautographic study on the uptake of $^{35}SO4$ in mouse ovary during the estrus cycle. J Clin Electron Microsc 1992;25:709-10.

Li S, Nagata T. Nucleic acid synthesis in the developing mouse ovary, uterus and oviduct studied by light and electron microscopic radioautography. Cell Mol Biol 1995;41:185-95.

Liang Y. Light microscopic radioautographic study on RNA synthesis in the adrenal glands of aging mice. Acta Histochem Cytochem 1998;31:203-10.

Liang Y, Ito M, Nagata T. Light and electron microscopic radioautographic studies on RNA synthesis in aging mouse adrenal gland. Acta Anat Nippon 1999;74:291-300.

Lillie R D. Various oil soluble dyes as fat stain in supersaturated isopropanol technic. Stain Technol 1944;19:55-8.

Ma H. Light microscopic radioautographic study on DNA synthesis of the livers in aging mice. Acta Anat Nippon 1988;63:137-47.

Ma H, Nagata T. Electron microscopic radioautographic study on DNA synthesis of the livers in aging mice. J Clin Electron Microsc 1988a;21:335-43.

Ma H, Nagata T. Studies on DNA synthesis of aging mice by means of electron microscopic radioautography. J Clin Electron Microsc 1988b;21:715-6.

Ma H, Nagata T. Electron microscopic radioautographic studies on DNA synthesis in the hepatocytes of aging mice as observed by image analysis. Cell Mol Biol 1990a;36:73-

84.

Ma H, Nagata T. Study on RNA synthesis in the livers of aging mice by means of electron microscopic radioautography. Cell Mol Biol 1990b;36:589-600.

Ma H, Nagata T. Collagen and protein synthesis in the livers of aging mice as studied by electron microscopic radioautography. Ann Microscopy 2000;1:13-22.

Ma H, Gao F, Olea M T, Nagata T. Protein synthesis in the livers of aging mice studied by electron microscopic radioautography. Cell Mol Biol 1991;37:607-15.

Momose Y, Naito J, Nagata T. Radioautographic study on the localization of an anti-allergic agent, tranilast, in the rat liver. Cell Mol Biol 1989;35:347-55.

Morita T. Radioautographic study on the aging change of ^{3}H-glucosamine uptake in mouse ileum. Cell Mol Biol 1993;39:875-84.

Morita T, Usuda N, Hanai T, Nagata T. Changes of colon epithelium proliferation due to individual aging with PCNA/cyclin immunostaining comparing with ^{3}H-thymidine radioautography. Histochemistry 1994a;101:13-20.

Morita T, Usuda N, Hanai T, Kong Y, Nagata T. Lectin histochemistry of the developing and aging mice colons. Acta Histochem Cytochem 1994b;24:527-7.

Murata F, Momose Y , Yoshida K, Nagata T. Incorporation of ^{3}H-thymidine into the nucleus of mast cells in adult rat peritoneum. Shinshu Med J 1977a;25:72-7.

Murata F, Momose Y, Yoshida K, Ohno S, Nagata T. Nucleic acid and mucosubstance metabolism of mastocytoma cells by means of electron microscopic radioautography. Acta Pharmacol Toxicol 1977b;41:58-9.

Murata F, Momose Y, Nagata T. Demonstration of intracytoplasmic glycogen of megakaryocytes and blood platelets by means of the periodic acid-thiocarbohydrazide-silver proteinate method. Histochemistry 1977c;52:307-16.

Murata F, Nagata T, Spicer S S. Fine structural localization of arylsulfatase B activity in the rabbit blood platelets. Histochemistry 1975;44:307-12.

Murata F, Yokota S, Nagata T. Electron microscopic demonstration of lipase in pancreatic acinar cells of mouse. Histochemie 1968;13:215-22.

Murata F, Yoshida K, Ohno S, Nagata T. Ultrastructural and electron microscopic radioautographic studies on the mastocytoma cells and mast cells. J Clin Electron Microsc 1978;11:561-2.

Murata F, Yoshida K, Ohno S, Nagata T. Mucosubstances of rabbit granulocytes studied by means of electron microscopic radioautography and X-ray microanalysis. Histochemistry 1979;61:139-50.

Nagata T. On the relationship between cell division and cytochrome oxidase in the Yoshida sarcoma cells. Shinshu Med J 1956;5:383-6.

Nagata T. Quantification of DNA contents in rat hepatocytes by means of microspectrophotometry, with special reference to binucleate cells. Arch Histol Japon 1961a;22:81-2.

Nagata T. A new method for preparing specimens suitable to micropectrophotometry of

binucleate cell nuclei stained with the Feulgen reaction. Med J Shinshu Univ 1961b;6:137-41.

Nagata T. A quantitative study of the DNA contents in rat hepatic cell nuclei by means of microspectrophotometry, with special reference to binucleate cells. Med J Shinshu Univ 1961c;6:143-53.

Nagata T. A radioautographic study of the DNA synthesis in rat liver, with special reference to binucleate cells. Med J Shinshu Univ 1962;7:17-25.

Nagata T. A quantitative study on the ganglion cells in the small intestine of the dog. Med J Shinshu Univ 1965;10:1-11.

Nagata T. Theory and application of microspectrophotometry: Introduction to quantitative histochemistry. Shinshu Med J 1966a;15:148-57.

Nagata T. A radioautographic study on the RNA synthesis in the hepatic and the intestinal epithelial cells of mice after feeding with special reference to binuclearity. Med J Shinshu Univ 1966b;11:49-61.

Nagata T. A radioautographic study on the protein synthesis in the hepatic and the intestinal epithelial cells of mice, with special reference to binucleate cells. Med J Shinshu Univ 1967;12:247-57.

Nagata T. Application of microspectrophotometry to various substances. In , Introduction to Microspectrophotometry. In: Isaka S, Nagata T, Inui N (eds.). Tokyo: Olympus Co;1972a:49-155.

Nagata T. Electron microscopic dry-mounting autoradiography. Proc 4th Internat Cong Histochem Cytochem Kyoto 1972b:43-4.

Nagata T. Chapter 7. Lipase, In: Hayat MA (ed.). Electron microscopy of enzymes, principles and methods. New York: Van Nostrand Reinhold Co.; 1974;2:132-48.

Nagata T. Electron microscopic radioautography and analytical electron microscopy. J Clin Electron Microscopy 1991;24:441-2.

Nagata T. Radiolabeling of soluble and insoluble compounds as demonstrated by light and electron microscopy. In: Wegmann R J, Wegmann M A (eds.). Recent Advances in Cellular and Molecular Biology. Vol. 6. Molecular Biology of Pyridines, DNA, Peroxisomes, Organelles and Cell Movements. Leuven, Belgium: Peeters Press, 1992; 9-21.

Nagata T. Quantitative analysis of histochemical reactions: Image analysis of light and electron microscopic radioautograms. Acta Histochem Cytochem 1993a;26:281-91.

Nagata T. Quantitative light and electron microscopic radioautographic studies on macromolecular synthesis in several organs of prenatal and postnatal aging mice. Chinese J Histochem Cytochem 1993b;2:106-8.

Nagata T. Electron microscopic radioautography with cryo-fixation and dry-mounting procedure. Acta Histochem Cytochem 1994a;27:471-89.

Nagata T. Application of electron microscopic radioautography to clinical electron microscopy. Med Electron Microscopy 1994b;27:191-212.

Nagata T. Radioautography in Medicine. Matsumoto: Shinshu University Press; 1994c.

Nagata T. Light and electron microscopic radioautographic study on macromolecular synthesis in digestive organs of aging mice. Cell Mol Biol 1995a;41:21-38.

Nagata T. Histochemistry of the organs; Application of histochemistry to anatomy. Acta Anat Nippon 1995b;70:448-71.

Nagata T. Three-dimensional observation of whole mount cultured cells stained with histochemical reactions by ultrahigh voltage electron microscopy. Cell Mol Biol 1995c;41:783-92.

Nagata T. Morphometry in anatomy: image analysis on fine structure and histochemical reactions with special reference to radioautography. Ital J Anat 1995d;100(Suppl.1):591-605.

Nagata T. Technique and application of electron microscopic radioautography. J Electron Microscopy 1996a;45:258-74.

Nagata T. Techniques of light and electron microscopic radioautography. In: JSHC (ed.). Histochemistry and Cytochemistry 1996. Proc. Xth Internat Congr Histochem Cytochem Kyoto, Acta Histochem Cytochem 1996b;29(Suppl.):343-4.

Nagata T. Introductory Remarks: Radioautographology, general and special. Cell Mol Biol 1996c;42(Suppl.):11-2.

Nagata T. Techniques and applications of microscopic radioautography. Histol Histopathol 1997a;12:1091-124

Nagata T. Three-dimensional observation on whole mount cultured cells and thick sections stained with histochemical reactions by high voltage electron microscopy. In: Motta P. (ed.). Recent Advances in Microscopy of Cells, Tissues and Organs, Roma: Antonio Delfino Editore; 1997b:37-44.

Nagata T. Radioautographic study on collagen synthesis in the ocular tissues. J Kaken Eye Res 1997c;15: 1-9.

Nagata T. Techniques of radioautography for medical and biological research. Braz J Biol Med Res 1998a;31:185-95.

Nagata T. Radioautographology, the advocacy of a new concept. Braz J Biol Med Res 1998b;31:201-41.

Nagata T. Radioautographic studies on DNA synthesis of the bone and skin of aging salamander. Bull Nagano Women's Jr College 1998c;6:1-14.

Nagata T. 3D observation of cell organelles by high voltage electron microscopy. Microscopy and Analysis, Asia Pacific Edition, 1999a;9:29-32.

Nagata T. Application of histochemistry to anatomy: Histochemistry of the organs, a novel concept. Proc XV Congress of the International Federation of Associations of Anatomists, Ital J Anat Embryo 1999b;104(Suppl.1): 486-6.

Nagata T. Aging changes of macromolecular synthesis in various organ systems as observed by microscopic radioautography after incorporation of radiolabeled precursors. Methods Find Exp Clin Pharmacol 1999c;21:683-706.

Nagata T. Radioautographic study on protein synthesis in mouse cornea. J Kaken Eye Res 1999d;8:8-14.

Nagata T. Three-dimensional observations on thick biological specimens by high voltage electron microscopy. Image Analysis Stereolog 2000a;19:51-6.

Nagata T. Biological microanalysis of radiolabeled and unlabeled compounds by radioautography and X-ray microanalysis. Scanning Microscopy International, Chicago, USA, 2000b;12:1-41.

Nagata T. Electron microscopic radioautographic study on protein synthesis in pancreatic cells of perinatal and aging mice. Bull Nagano Women's Jr College 2000c; 8:1-22.

Nagata T. Light microscopic radioautographic study on radiosulfate incorporation into the tracheal cartilage in aging mice.Acta Histochem Cytochem 2000d;32:377-83.

Nagata T. Application of histochemical techniques to observe 3-dimensional structure of cell organelles in thick specimens by high voltage electron microscopy. Chin J Histochem Cytochem 2000e;9(Suppl):21-2.

Nagata T. Special radioautographology: the eye. J Kaken Eye Res 2000f;18:1-13.

Nagata T. Three-dimensional high voltage electron microscopy of thick biological specimens. Micron 2001a;32:387-404.

Nagata T. Three-dimensional and four-dimensional observation of histochemical and cytochemical specimens by high voltage electron microscopy. Acta Histochem Cytochem 2001b;34:153-69.

Nagata T. Special cytochemistry in cell biology. In: Jeon KW (ed.). Internat Rev Cytol New York: Academic Press; 2001c;211:33-154.

Nagata T. Aging changes of macromolecular synthesis in the respiratory organs as revealed by microscopic radioautography. ARBS Ann Rev Biomed Sci 2001d;3:127-55.

Nagata T. Radioautographology, General and Special. In: Graumann W (ed.). Prog Histochem Cytochem. Jena: Urban & Fischer; 2002a;37(2):57-228.

Nagata T. Aging changes of macromolecular synthesis in the digestive organs of mice as revealed by microscopic radioautography and X-ray microanalysis. ARBS Ann Rev Biomed Sci 2002b;4:79-132.

Nagata T. Aging changes of macromolecular synthesis in various organs as revealed by electron microscopic radioautography. In: Nagayama K. (ed.), Proc 30th NIPS International Symposium, Frontiers of Biological Electron Microscopy - Proteins to Supramolecules. Okazaki: National Institute for Physiological Sciences, Okazaki National Research Institute; 2003a:144-5.

Nagata T. Morphodynamics of macromolecular synthesis in various cells, tissues and organs as revealed by light and electron microscopic radioautography. Proc 5th International Malpighi Symposium, Rome, Ital J Anat Embryol 2003b;108(Suppl1):98-8.

Nagata T. Light and electron microscopic radioautographic studies on macromolecular synthesis in amitotic hepatocytes of aging mice. Cell Mol Biol 2003c;49:591-611.

Nagata T. The utility value of high voltage electron microscopy for X-ray microanalysis. Acta Histochem Cytochem 2003d;36:299-315.

Nagata T. Recent advances in cytochemical methodology in medical and biological sciences. SBPN Scientific J. 2004a;1:5-20.

Nagata T. X-ray microanalysis of biological specimens by high voltage electron microscopy. In: Sasse D (ed). Prog Histochem Cytochem, Jena: Elsevier; 2004b:39(4):15-320.

Nagata T. Principle and application of X-ray microanalysis to biological specimens by high voltage electron microscopy. ARBS Ann Rev Biomed Sci 2004c;6:13-78.

Nagata T. Electron microscopic radioautography of intramitochondrial nucleic acid synthesis in mouse hepatocytes**.** Proc 8th Asia-Pacific Conference on Electron Microscopy (8APEM), Kanazawa: Jap Soc Microsc; 2004d:1231-32.

Nagata T. Introductory remarks to symposium "Special Histochemistry: Histochemistry of the organs - Application of histochemistry to special histology" Proc. 16th Internat. Cong. of IFAA (International Federation of Associations of Anatomists), Kyoto, Japan, p. 193-94, 2004e

Nagata T, Cui H, Gao F. Radioautographic study on glycoprotein synthesis in the ocular tissues. J Kaken Eye Res 1995;13:11-18.

Nagata T, Cui H, Kong Y. The localization of TGF-b1 and its mRNA in the spinal cords of prenatal and postnatal aging mice demonstrated with immunohistochemical and in situ hybridization techniques. Bull Nagano Women's Jr College 1999b;7:75-88.

Nagata T, Fujiwara I, Shimamura K. On the argentaffine reaction of melanins and their precursors. Shinshu Med J 1957a;6:515-17.

Nagata T, Fujiwara I, Shimamura K. On the distribution of calcium in the stratified squamous epithelia. Acta Anat Nippon 1957b;32:305-10.

Nagata T, Hirano I, Shibata O, Nagata T. A radioautographic study on the DNA synthesis in the hepatic and the pancreatic acinar cells of mice during the postnatal growth, with special reference to binuclearity. Med J Shinshu Univ 1966;11:35-42.

Nagata T, Ito M, Chen S. Aging changes of DNA synthesis in the submandibular glands of mice as observed by light and electron microscopic radioautography. Ann Microsc 2000a;1:4-12.

Nagata T, Ito M, Liang Y. Study of the effects of aging on macromolecular synthesis in mouse steroid secreting cells using microscopic radioautography. Methods Find Exp Clin Pharmacol 2000b;22:5-18.

Nagata T, Iwadare N. Electron microscopic demonstration of phospholipase B activity in the liver and the kidney of the mouse. Histochemistry 1984;80:149-52.

Nagata T, Kametani K. X-ray microanalysis of various elements in biological specimens by high voltage electron microscopy. Proc 8th Asia-Pacific Conference on Electron Microscopy (8APEM), Kanazawa: Jap Soc Microsc;2004:1101-2.

Nagata T, Kametani K, Maruyama M. X-ray microanalysis of sulfur in cryo-fixed colonic goblet cells by high voltage electron microscopy. Scanning Microscopy 1998;14:1-12.

Nagata T, Kawahara I. Radioautographic study of the synthesis of sulfomucin in digestive organs of mice. J Trace Microprobe Analysis 1999;17:339-55.

Nagata T, Kawahara I, Usuda N, Maruyama M, Ma H. Radioautographic studies on the glycoconjugate synthesis in the gastrointestinal mucosa of the mouse. In: Ohyama M, Muramatsu T (eds). Glycoconjugate in Medicine, Tokyo: Professional Postgrad Service;1988a:251-6.

Nagata T, Kong Y. Distribution and localization of TGFb1 and bFGF, and their mRNAs in aging mouse eye. Bull Nagano Women's Junior College 1998;6:87-105.

Nagata T, Kong Y. Histochemical studies on the age-related changes in glycoconjugates of mouse ocular tissues as shown by lectin binding patterns. Bull. Nagano Women's Jr College 2000;8:109-29.

Nagata T, Ma H. Electron Microscopic Radioautographic Study On the Macromolecular Synthesis in Binucleate Hepatocytes Of Aging Mouse. Ann Microscopy 2003a;3:53-68.

Nagata T, Ma H. Electron microscopic radioautographic study on nucleic acid synthesis in amitotic hepatocytes of aging mouse. Med Electron Microsc 2003b;36:263-71.

Nagata T, Matsumura K. Radioautographic studies on DNA synthesis of the lungs of aging salamanders. Ann Microscopy 2004;4:4-13.

Nagata T, Morita T, Kawahara I. Radioautographic studies on radiosulfate incorporation in the digestive organs of mice. Histol Histopathol 1999a;14:1-8.

Nagata T, Murata F. Electron microscopic dry-mounting radioautography for diffusible compounds by means of ultracryotomy. Histochemistry 1977;54:75-82.

Nagata T, Murata F. Esterase, In: Takeuchi T, Ogawa K (eds.). Enzyme histochemistry, Tokyo: Asakura Shoten; 1980:225-53.

Nagata T, Nawa T. A modification of dry-mounting technique for radioautography of water-soluble compounds. Histochemie 1966a;7:370-1.

Nagata T, Nawa T. A radioautographic study on the nucleic acids synthesis of binucleate cells in cultivated fibroblasts of chick embryos. Med J Shinshu Univ 1966b;11:1-5.

Nagata T, Nawa T, Yokota S. A new technique for electron microscopic dry-mounting radioautography of soluble compounds. Histochemie 1969;18:241-9.

Nagata T, Nishigaki T, Momose Y. Localization of anti-allergic agent in rat mast cells demonstrated by light and electron microscopic radioautography. Acta Histochem cytochem 1986;19:669-83.

Nagata T, Ohno S, Murata F. Electron microscopic dry-mounting radioautography for soluble compounds. Acta Pharmacol Toxicol 1977;41:62-3.

Nagata T, Olea MT. Electron microscopic radioautographic study on the protein synthesis in aging mouse spleen. Bull Nagano Women's Jr College 1999;7:1-9.

Nagata T, Shibata O, Nawa T. Incorporation of tritiated thymidine into mitochondrial DNA of the liver and kidney cells of chickens and mice in tissue culture. Histochemie 1967;10:305-8.

Nagata T, Shibata O, Omochi S. A new method for radioautographic observation on isolated cells. Histochemie 1961;2:255-9

Nagata T, Shimamura K. Radioautographic studies on calcium absorption. I. Calcium absorption in the stomach of rat. Med J Shinshu Univ 1958;3:83-90.

Nagata T, Shimamura K. Radioautographic studies on calcium absorption. II. Calcium absorption in the intestines of rat. Med J Shinshu Univ 1959a;4:1-10.

Nagata T, Shimamura K. Radioautographic studies on calcium absorption. III. Distribution of radiocalcium in the liver and the kidney of rat after oral administration. Med J Shinshu Univ 1959b;4:11-8.

Nagata T, Toriyama K, Kong Y, Jin C, Gao F. Radioautographic study on DNA synthesis in the ciliary bodies of aging mice. J Kaken Eye Res 1994;12:1-11.

Nagata T, Usuda N. Image processing of electron microscopic radioautograms in clinical electron microscopy. J Clin Electron Microsc 1985;18:451-2.

Nagata T, Usuda N. Studies on the nucleic acid synthesis in pancreatic acinar cells of aging mice by means of electron microscopic radioautography. J Clin Electron Microsc 1986;19:486-7.

Nagata T, Usuda N. Electron microscopic radioautography of protein synthesis in pancreatic acinar cells of aging mice. Acta Histochem Cytochem 1993a;26:481-2.

Nagata T, Usuda N. In situ hybridization by electron microscopy using radioactive probes. J Histochem Cytochem 1993b;41:1119.

Nagata T, Usuda N, Ma H. Electron microscopic radioautography of nucleic acid synthesis in pancreatic acinar cells of prenatal and postnatal aging mice. Proc XIth Intern Cong Electron Microsc 1984;3:2281-2.

Nagata T, Usuda N, Ma H. Studies on the nucleic acid synthesis in pancreatic acinar cells of aging mice by means of electron microscopic radioautography. J Clin Electron Microsc 1986;19:486-7.

Nagata T, Usuda N, Ma H. Electron microscopic radioautography of lipid synthesis in pancreatic cells of aging mice. J Clin Electron Microsc 1990;23:841-2.

Nagata T, Usuda N, Maruyama M, Ma H. Electron microscopic radioautographic study on lipid synthesis in perinatal mouse pancreas. J Clin Electron Microsc 1988b;21:756-7.

Nagata T, Usuda N, Suzawa H, Kanzawa M. Incorporation of ^{3}H-glucosamine into the pancreatic cells of aging mice as demonstrated by electron microscopic radioautography. J Clin Electron Microsc 1992;25:646-7.

Nagata T, Yoshida K, Murata F. Demonstration of hot and cold mercury in the human thyroid tissues by means of radioautography and chemography. Acta Pharmacol 1977b;41:60-1.

Nawa T, Nagata T, Omochi S. An apparatus for freeze-drying of tissue. Med J Shinshu Univ 1965;10:1-11.

Nawa T, Nagata T, Tokota S, Murata F, Omochi S. Two new models of freeze-drying

apparatus for tissues. Med J Shinshu Univ 1969;14:1-15.

Nishigaki T, Momose Y, Nagata T. Light microscopic radioautographic study of the localization of anti-allergic agent, Tranilast, in rat mast cells. Histochem J 1987;19:533-6.

Nishigaki T, Momose Y, Nagata T. Localization of the anti-allergic agent tranilast in the urinary bladder of rat as demonstrated by light microscopic radioautography. Drug Res 1990;40:272-5.

Ohno S. Peroxisomes of the kidney. In: Bourne GH, Danielli JF, Jeon KW (eds.). Internat Rev Cytol New York: Academic Press. 1985;95:131-62.

Ohno S, Murata F, Yoshida K, Tei I, Nagata T. Ultrastructural changes of rat kidneys treated with DEHP. J Clin Electron Microsc 1978;11:841-2.

Ohno S, Ohtake N, Fujii Y, Yamabayashi S, Usuda N, Nagata T. Histochemical studies on peroxisomes of rat livers during DEHP administration and after withdrawal of thick sections by means of light microscopic and high voltage electron microscopy. Acta Histochem Cytochem 1981;14:125-42.

Ohno S, Fujii Y, Usuda N, Murata F, Nagata T. Peroxisome proliferation of rat kidney induced with DEHP. I. Numerical changes by light microscopic morphometry. Acta Histochem Cytochem 1982;15:40-57.

Olea MT. Ultrastructural localization of lysosomal acid phosphatase activity in aging mouse spleen: a quantitative X-ray microanalytical study. Acta Histochem Cytochem 1991;24:201-8.

Olea M T, Ma H, Nagata T. Quantitative assessment of lysosomal size, number and enzyme activity in mouse kidney during maturational development. Cell Mol Biol 1991a;37:679-85.

Olea M T, Nagata T. X-ray microanalysis of cerium in mouse spleen cells demonstrating acid phosphatase activity using high voltage electron microscopy, Cell Mol Biol 1991b;37:155-63.

Olea MT, Nagata T. Simultaneous localization of ^{3}H-thymidine incorporation and acid phosphatase activity in mouse spleen: EM radioautography and cytochemistry. Cell Mol Biol 1992a;38:115-22.

Olea MT, Nagata T. A radioautographic study on RNA synthesis in aging mouse spleen after ^{3}H-uridine labeling *in vitro*. Cell Mol Biol 1992b;38:399-405.

Olea MT, Nagata T. Application of high voltage electron microscopy to electron microscopic radioautography: A study on the protein synthesis in aging mouse spleen labeled with ^{3}H-leucine. Ann Microsc 2003;3:69-83.

Oliveira SF, Nagata T, Abrahamsohn PA, Zorn TMT. Electron microscopic radioautographic study on the incorporation of ^{3}H-proline by mouse decidual cells. Cell Mol Biol 1991;37:315-23.

Oliveira SF, Abrahamsohn PA, Nagata T, Zorn TMT. Incorporation of ^{3}H-amino acids by endometrial stromal cells during decidualization in the mouse. A radioautographical

study. Cell Mol Biol 1995;41:107-16.

Paffaro VA Jr, Bizinotto MC, Joazeiro PP, Yamada AT. Subset classification of mouse uterine natural killer cells by DBA lectin reactivity. Placenta 2003;24:479-88.

Patonai A, Csikos A, Deak G. Visceral aluminum deposition in chronic renal insufficiency. (Light microscopy and X-ray microanalysis). Pathol Oncol Res 1996;2:94-7.

Pearse AGE. Histochemistry, theoretical and applied. 1st ed. Little Brown Co. Boston, 1953

Pearse AGE. Histochemistry, theoretical and applied. 2nd ed. Little Brown Co. Boston, 1958

Przelecka A, Mrozinska K. Calcium-cadmium competition in ovarian vitellogenic follicles of Galleria mellonella as revealed by X-ray microanalysis. Folia Histochem Cytobiol 2002;40:229-30.

Roth J. The colloidal gold marker system for light and electron microscopic cytochemistry. In: Bullock GR, Petrusz P. (eds.), Techniques in Immunocytochemistry. London, NY Academic Press; 1983;2: 217-84.

Roth J, Binder M. Colloidal gold, ferritin and peroxidase for electron microscopic double labeling lectin technique. J Histochem Cytochem 1978;26:163-9.

San Martin S, Soto-Suazo M, Ferreira de Oliveira S, Aplin JD, Abrahamsohn PA, Zorn TMT. Small leucine-rich proteoglycans (SLRPs) in uterine tissues during pregnancy in mice. Reproduction 2003a;125:585-95.

San Martin S, Soto-Suazo M, Zorn TMT. Versican and hyaluronan in the mouse uterus during decidualization. Braz J Med Biol Res 2003b;36:1067-71.

Sato A. Quantitative electron microscopic studies on the kinetics of secretory granules in G-cells. Cell Tissue Res 1978;187:45-59.

Sato A, Iida F, Furihata R, Nagata T. Electron microscopic radioautography of rat stomach G-cells by means of ^{3}H-amino acids. J Clin Electron Microsc 1977;10:358-9.

Sauren YMHF, Mierement RHP, Groot CG, Scherfft JP. Polyethylen imine as a contrast agent for ultrastructural localization and characterization of proteoglycans in the matrix of cartilage and bone. J Histochem Cytochem 1991;39:331-40.

Scott G H, Horning H. Microincineration of tissues. In: Scott G H, Horning H (eds). Cytology and Cell Physiology, 2nd ed., Oxford: Oxford Press; 1953:15-36.

Sharon N, Lis H. Lectins: cell agglutinating and sugar specific proteins. Science 1972;177:949-59.

Spencer A J, Wood J A, Saunders H C, Freeman M S, Lote C J. Aluminum deposition in liver and kidney following acute intravenous administration of aluminum chloride or citrate in conscious rats. Hum Exp Toxicol 1995;14:787-94.

Sun L. Age related changes of RNA synthesis in the lungs of aging mice by light and electron microscopic radioautography. Cell Mol Biol 1995;41:1061-72.

Sun L, Gao F, Duan H, Nagata T. Light microscopic radioautography of DNA synthesis in pulmonary cells in aging mice. In: Nagata T. (ed.), Radioautography in Medicine,

Matsumoto: Shinshu University Press; 1994,201-5.

Sun L, Gao F, Nagata T. Study on the DNA synthesis of pulmonary cells in aging mice by light microscopic radioautography. Cell Mol Biol 1995a;41:851-9.

Sun L, Gao F, Jin C, Duan H, Nagata T. An electron microscopic radioautographic study on the DNA synthesis of pulmonary tissue cells in aging mice. Med Electron Microsc 1995b;28:129-31.

Sun L, Gao F, Jin C, Nagata T. DNA synthesis in the tracheae of aging mice by means of light and electron microscopic radioautography. Acta Histochem Cytochem 1997a;30:211-20.

Sun L, Gao F, Nagata T. A Light Microscopic Radioautographic Study on Protein Synthesis in Pulmonary Cells of Aging Mice. Acta Histochem Cytochem 1997b;30:463-70.

Takamatsu H. Morphological study on alkaline phosphatase. Manchurian Med J 1938;29:1351-1.

Takamatsu H. Morphological demonstration of alkaline phosphatase . Trans Soc Pathol Jap 1939:29;492-3.

Takaya K, Masuda T. Quantitative X-ray microanalysis of biological materials on freeze-dried stamps and fresh frozen dried ultrathin sections. J Clin Electron Microsc 1991;24:445-6.

Terauchi A, Mori T, Kanda H, Tsukada M, Nagata T. Radioautographic study of ^{3}H-taurine uptake in mouse skeletal muscle cells. J Clin Electron Microsc 1988;21:627-8.

Terauchi A, Nagata T. Observation on incorporation of ^{3}H-taurine in mouse skeletal muscle cells by light and electron microscopic radioautography. Cell Mol Biol 1993;39:397-404.

Terauchi A, Nagata T. In corporation of ^{3}H-taurine into the blood capillary cells of mouse skeletal muscle. In: Nagata T. (ed), Radioautography in Medicine. Matsumoto: Shinshu University Press, 1994;155-9.

Thiéry JP. Mise en evidence des polysaccharides sur coupes fines en microscopie electronique. J Microsc 1967;6:987-1018.

Toriyama K. Study on the aging changes of DNA and protein synthesis of bipolar and photo-receptor cells of mouse retina by light and electron microscopic radioautography. Cell Mol Biol 1995;41:593-601.

Usuda N, Hanai T, Morita T, Nagata T. Radioautographic demonstration of peroxisomal acyl-CoA oxidase mRNA by in situ hybridization. In: Wegmann R J, Wegmann M. (eds.), Recent advances in cellular and molecular biology. Leuven: Peeters Press, Vol. 6. Molecular biology of nucleus, peroxisomes, organelles and cell movement. 1992;181-4.

Usuda N, Nagata T. Immunohistochemical characterization of microperoxisomes of small intestinal epithelial cells. Acta Histochem Cytochem 1984;17:726-6.

Usuda N, Nagata T. Post-embedding immunoelectron microscopy of tissues processed by rapid freezing and freeze-substitution without chemical fixatives. Authors' response. J

Histochem Cytochem 1991;39:546-7.

Usuda N, Nagata T. Electron microscopic radioautography of acyl-CoA mRNA by in situ hybridization. J Clin Electron Microsc 1992;25:332-3.

Usuda N, Nagata T. The immunohistochemical and in situ hybridization studies on hepatic peroxisomes. Acta Histochem Cytochem 1995;28:169-72.

Usuda N, Kameko M, Kanai T, Nagata T. Immunocytochemical demonstration of retinol-binding protein in the lysosomes of the proximal tubules of the human kidney. Histochemistry 1983;78:487-90.

Usuda N, Yokota S, Hashimoto T, Nagata T. Immunohistochemical localization of D-amino acid oxidase in the central clear matrix of rat kidney peroxisomes. J Histochem Cytochem 1986;34:1709-18.

Usuda N, Ma H, Hanai T, Yokota S, Hashimoto T, Nagata T. Immunoelectron microscopy of tissues processed by rapid freezing and freeze-substitution without chemical fixatives. Application to catalase in rat liver hepatocytes. J Histochem Cytochem 1990;38:617-23.

Usuda N, Kong Y, Hagiwara M, Uchida C, Terasawa M, Nagata T, Hidaka H. Differential localization of protein kinase C in retinal neurons. J Cell Biol 1991a;112:1241-7.

Usuda N, Kuwabara T, Ichikawa R, Hashimoto T, Nagata T. Immunoelectron microscopic evidence for organ difference in the composition of peroxisome-specific membrane polypeptides among three rat organs: Liver, kidney and intestine. J Histochem Cytochem 1991b;39:1357-66.

Usuda N, Yokota S, Ichikawa R, Hashimoto T, Nagata T. Immunoelectron microscopic study of a new D-amino acid oxidase-immunoreactive subcompartment in rat liver peroxisomes. J Histochem Cytochem 1991c;39:95-102.

Usuda N, Hayashi S, Fujiwara S, Noguchi T, Nagata T, Rao M S, Alvares K, Reddy JK, Yeldandi AB Uric acid degrading enzymes, urate oxidase and allantoinase, are associated with different subcellular organelles in frog liver and kidney. J Cell Sci 1994;107:1073-91.

Usuda N, Hanai T, Nagata T. Immunogold studies on peroxisomes: Review of the localization of specific proteins in vertebrate peroxisomes. Microsc Res Tech 1995;31:79-92.

Usuda N, Nakazawa A, Terasawa M, Reddy JK, Nagata T. Immunocytochemical study of the ultrastructure of peroxisomes and the effects of peroxisome proliferators. In: Reddy J K, Suga T, Mannaerts G P, Lazarow P B, Subramani S. (eds.), Peroxisomes, biology and role in toxicology and disease. Ann. N.Y. Acad. Sci. USA, 1996;804:297-309.

Watanabe I, Makiyama MCK, Nagata T Electron microscopic radioautographic observation of the submandibular salivary gland of aging mouse. Acta Microscopica 1997;6:130-1.

Watanabe I, Nagata T. Changes of glucide synthesis in the submandibular glands of aging

mice as observed by light and electron microscopic radioautography. Ann Microsc 2001;2:4-15.

Yamada AT. Timely and topologically defined protein synthesis in the periimplanting mouse endometrium revealed by light and electron microscopic radioautography. Cell Mol Biol 1993;39:1-12.

Yamada AT, Copi C, Joazeiro PP. Histochemical and immunocytochemical study of uNK cells in the non-pregnant and normal or abnormal pregnant mice. Proc 16th Internat Cong IFAA, Anat Sci Internat 2004;79(Suppl):196-6.

Yamada AT, Nagata T. Ribonucleic acid and protein synthesis in the uterus of pregnant mouse during activation of implantation window. Med Electron Microsc 1992a;27:363-65.

Yamada AT, Nagata T. Light and electron microscopic radioautography of DNA synthesis in the endometria of pregnant-ovariectomized mice during activation of implantation window. Cell Mol Biol 1992b;38:763-74.

Yamada AT, Nagata T. Light and electron microscopic radioautography of RNA synthesis of peri-implanting pregnant mouse during activation of receptivity for blastocyst implantation. Cell Mol Biol 1993;38:211-33.

Yokota S, Nagata T. Study on mouse liver urate oxidase. III. Fine localization of urate oxidase in liver cells revealed by means of ultracryotomy-immunoferritin method. Histochemistry 1973;39:243-50.

Yokota S, Nagata T. Ultrastructural localization of catalase on ultracryotomic sections of mouse liver by ferritin-conjugated antibody technique. Histochemistry 1974;40:165-74.

Yokota S, Nagata T. Chapter 5. Urate oxidase, In: Hayat MA (ed.), Electron microscopy of enzymes, Principles and methods. New York: Van Nostrand Reinhold Co.; 1977:5;72-97.

Yoshinaga K. Uterine receptivity for blastcyst implantation. Ann. N. Y. Acad. Sci. USA, 1988; 541: 424-31.

Yoshizawa S, Nagata A, Honma T, Oda M, Murata F, Nagata T.: Study of ethionine pancreatitis by means of electron microscopic radioautography. J Clin Electron Microsc 1974;7:349-50.

Yoshizawa S, Nagata A, Honma T, Oda M, Murata F, Nagata T. Radioautographic study of protein synthesis in pancreatic exocrine cells of alcoholic rats. J Clin Electron Microscopy 1977;10:372-3.

Zorn T M T, San Martin S. Histochemical and immunocytochemical characterization of the extracellular matrix of mouse endometrium during pregnancy. Proc 16th Internat Cong IFAA, Anat Sci Internat 2004;79(Suppl):196-6.